Environmental Impact Assessment Review 121 (2026) 108582

Contents lists available at ScienceDirect

Environmental Impact Assessment Review

journal homepage: www.elsevier.com/locate/eiar

# Modular multi-domain AI framework for sustainable construction material optimisation

Asal Pournaghshband [a], Farzad Piadeh [a,*], Mohsen Ahmadi [b], Ayda Sahaf [c]

[a] Centre for Engineering Research, School of Physics, Engineering and Computer Science, University of Hertfordshire, Hatfield AL10 9AB, UK
[b] School of Architecture and Built Environment, Deakin University, Geelong, VIC 3220, Australia
[c] MURi Consulting Group Inc., #3807 – 1480 Howe Street, Vancouver, BC V6Z 0G5, Canada

ARTICLE INFO

*Keywords:*
Artificial intelligence
Circularity
Embodied carbon
Life-cycle assessment
Material optimisation
Sustainable construction

ABSTRACT

The construction sector is a major contributor to global environmental impacts, largely driven by the embodied emissions of structural materials. Early-stage material selection therefore represents a critical opportunity for impact reduction; however, conventional life-cycle assessment (LCA) approaches remain limited in systematically evaluating large numbers of feasible material configurations under multiple and often conflicting sustainability criteria, constraining effective decision-making during design. To address this limitation, this study develops an artificial intelligence–driven decision-support framework for the systematic exploration and optimisation of construction material configurations within a fixed building design. The framework integrates LCA modelling, scenario-based material substitution, predictive modelling using mixture-of-experts backpropagation neural networks, and sustainability-oriented optimisation within a unified workflow. A reinforced-concrete office building in the United Kingdom is used as a case study to generate 1500 technically feasible material scenarios by varying concrete compositions (including GGBS and fly ash substitution), reinforcement steel production routes, cement formulations, and end-of-life pathways. Scenario outputs from OneClick LCA are used to train the predictive models, enabling rapid estimation of multiple sustainability indicators, which are subsequently coupled with a shuffled frog leaping optimisation algorithm using a composite sustainability index. The results demonstrate that the framework efficiently identifies material configurations that balance environmental, circularity, and cost-related performance while expanding the range of feasible design solutions beyond conventional scenario-based evaluation. The proposed framework provides a scalable and flexible decision-support tool for early-stage design, enabling systematic assessment of trade-offs and supporting informed material selection under practical design and feasibility constraints.

## 1. Introduction

The construction sector is a major contributor to global environmental impacts, driven by its intensive consumption of energy and raw materials throughout the building life cycle (Liu and Qian, 2019; Ahmadi et al., 2024). At the same time, the sector plays a critical role in societal development by delivering infrastructure that underpins economic activity and enhances quality of life (Alwan et al., 2017; Ajayi et al., 2025). In this context, life cycle assessment (LCA) and life cycle costing (LC) have emerged as a well-established and systematic framework for quantifying key environmental impacts, including global warming potential (GW), acidification (AC), resource depletion, and energy use, thereby supporting sustainability-driven decision-making in the construction industry (Dinh et al., 2020; Sabet et al., 2025).

At the application level, LCA–LC studies on construction and demolition waste management show that selective demolition combined with high-quality recycling significantly reduces GW and resource depletion compared with downcycling and landfill scenarios (Maria et al., 2018; Devaki and Shanmugapriya, 2022; Dong et al., 2023). Beyond waste management practices, the selection of construction systems and materials plays a critical role in shaping environmental impacts across the entire building life cycle (AbouHamad and Abu-Hamd, 2019; Barbhuiya and Das, 2023). Furthermore, extending the assessment beyond end-of-life (EoL) strategies at the building level can significantly influence key impact categories, including GW, AC, and eutrophication (EU) (Ghaffarianhoseini et al., 2021).

* Corresponding author.
*E-mail address:* f.piadeh@herts.ac.uk (F. Piadeh).

https://doi.org/10.1016/j.eiar.2026.108582
Received 16 March 2026; Received in revised form 16 June 2026; Accepted 21 June 2026
Available online 25 June 2026

However, despite these advances, significant limitations remain in design-stage LCA application. In practice, feasible design alternatives are constrained by extensive data requirements. These include time-intensive material substitution, evaluation of multiple EoL strategies, and modelling of numerous scenarios (Hassan Khan et al., 2025; Plociennik et al., 2025). These demands introduce high data and methodological complexity, which hampers scalable and consistent application (Häfliger et al., 2017). Additional challenges include interoperability issues, dependence on material classification systems, and limited coverage of multiple environmental indicators (Ghaffarianhoseini et al., 2021; Drewniok et al., 2023). As a result, designers are frequently restricted to a narrow set of material options for a given design layout (Nouri and Hu, 2025; Sesana et al., 2026).

Even recent LCA innovations that leverage automated and digital design environments – such as building information modelling (BIM)-based workflows (Guo et al., 2025), BIM-based decision models for alternative load-bearing structural systems (Vilutiene et al., 2020), Revit-based configurations (Hernández et al., 2023; Lima et al., 2024), and using commercial platforms such as OneClickLCA (Carvalho et al., 2021; Ahmadi et al., 2025) - remain predominantly evaluative in nature. These approaches have improved data integration and reduced manual input requirements, enhancing the efficiency and consistency of LCA workflows and enabling comparative analysis of design alternatives, with reported reductions in data - processing effort and improved transparency in environmental assessment. However, their application is largely limited to scenario-based comparisons, such as identifying up to 30–40% variations in embodied impacts across alternative structural systems or achieving up to 36% reductions through circular design strategies. Although recent modelling and BIM-integrated approaches have improved data availability and automation, they remain primarily assessment-driven (Huang et al., 2025 with limited capability to provide continuous feedback or enable optimisation-oriented modelling for guiding early-stage design decisions toward minimum-impact solutions.

To enable exploration of more diverse design scenarios, several decision-support approaches have been proposed, including the use of multi-criteria sustainability indicators, optimisation techniques, predictive models, and uncertainty-informed assessments to support comparison of alternatives and management of trade-offs during design (Serrano-Baena et al., 2023; Parece et al., 2025a, 2025b; Valipour et al., 2025). These approaches have demonstrated the ability to improve decision transparency and capture multi-dimensional sustainability performance, with reported reductions in embodied impacts and costs (e.g., up to 24–49% reductions in emissions and waste, and significant cost savings), as well as improved environmental performance through optimised material selection (e.g., ~30% carbon reduction). However, these approaches remain limited, as they primarily rely on predefined alternatives or case-specific scenarios and do not support systematic evaluation of a comprehensive range of material combinations within a fixed design configuration, nor enable continuous, large-scale exploration of the design space. The second approach employs optimisation-based modelling frameworks, yet only a limited number of studies explicitly integrate LCA and LC at the core of the design process. Within this category, the existing body of work remains sparse. For example, Gachkar et al. (2025) focused on improving automated and efficient data integration using supervised learning techniques, achieving high matching accuracy and reducing manual processing time by up to 90%, thereby enabling scalable and real-time LCA workflows for construction decision-making. Iqbal et al. (2025) nvestigated weak-learner artificial intelligence (AI) models to predict and optimise the environmental impacts of different building types, demonstrating high predictive accuracy and enabling early-stage design optimisation with 10–20% reductions in both life-cycle impacts and costs. Meanwhile, Yadav et al. (2025) employed hybrid deep learning coupled with genetic algorithms to identify solutions that balance high structural performance with reduced carbon footprints, achieving up to 30–35% reductions in $CO_2$ emissions and 10–15% cost savings while maintaining structural strength, highlighting the potential of multi-objective optimisation for sustainable material design.

Despite these advances, existing studies remain fragmented in the way they support design-stage decision-making. Dai (2026) highlighted that current building LCA studies remain affected by inconsistent system boundaries, inventory data, impact categories, and limited integration of broader sustainability dimensions, which restricts their ability to provide definitive design guidance. Similarly, Piadeh and Pournaghshband (2026) showed that AI has increasing potential for circularity assessment, lifecycle-related prediction, resource recovery, and decision support; however, existing applications remain constrained by data limitations, transferability issues, and insufficient integration into holistic circularity-assessment frameworks. In optimisation-based building LCA, Mohtashami et al. (2026) further demonstrated that case-based LCA scenarios may identify the best option only among predefined alternatives, whereas optimisation-based LCA is required to search a wider solution space and identify near-optimal cost–emission efficient solutions. These studies collectively show that the material-selection problem cannot be treated as a simple linear LCA calculation, because interactions among material categories, manufacturing routes, recycled content, EoL pathways, and sustainability indicators generate a combinatorial and multi-dimensional decision space. This limitation is also confirmed by the recent systematic review of BIM-based LCA by Parece et al. (2025a, 2025b), who emphasised that BIM-LCA research has progressed in automation, data extraction, and environmental assessment, but remains less developed in supporting actual design decision-making.

Their review identifies decision-support capabilities such as multi-criteria evaluation, multi-objective optimisation, predictive modelling, and sensitivity or uncertainty analysis as essential for translating LCA results into design decisions. In this context, the key gap is not only the calculation of environmental impacts, but the lack of integrated frameworks able to generate alternatives, evaluate multiple sustainability indicators, capture trade-offs, and guide designers toward improved solutions during early-stage design. Therefore, an integrated AI-assisted LCA decision-support framework is required to move beyond predefined scenario comparison and enable systematic optimisation of feasible material configurations within a fixed building design. It should be noted that the underlying life-cycle assessment calculations employed in this study remain fundamentally linear and are performed using established LCA procedures. The motivation for introducing AI is therefore not to replace or improve the numerical calculation of LCIA indicators themselves. Rather, the challenge addressed here arises from the combinatorial nature of the material-selection problem, where multiple material families, recycled-content levels, manufacturing routes, and end-of-life pathways interact to generate a large number of feasible design configurations. Consequently, the contribution of the proposed framework lies in supporting systematic exploration, evaluation, and optimisation of this design space rather than replacing conventional LCA calculations.

A major limitation of existing approaches lies in the absence of an integrated decision-support framework (DSF) capable of systematically guiding material selection under multiple, interdependent, and often conflicting sustainability objectives (Moustafa et al., 2026). Current LCA-based approaches are predominantly assessment-oriented, relying on retrospective evaluation of predefined scenarios rather than actively supporting the generation and optimisation of alternative design configurations (Aghdam and Dixit, 2026; Shi et al., 2026). Consequently, they provide limited capability for identifying optimal material combinations within large and complex design spaces. An effective DSF is therefore required to generate, evaluate, and rank feasible alternatives while explicitly accounting for trade-offs among environmental impacts, circularity potential, and economic performance.

A further challenge emerges when such frameworks are applied to large combinatorial material-design spaces. Although LCA provides a rigorous basis for sustainability assessment, each candidate material

configuration must be evaluated across multiple environmental, circularity, and economic indicators. As the number of feasible combinations increases, repeated execution of full LCA calculations becomes computationally demanding, particularly when embedded within iterative optimisation and scenario-generation procedures. This computational burden restricts practical exploration of large solution spaces and limits the scalability of optimisation-driven decision-support frameworks. To overcome this limitation, increasing attention has been directed toward integrated AI–LCA frameworks, where AI-based predictive models function as computationally efficient surrogate evaluators of sustainability performance. Such integration enables rapid assessment of large numbers of material configurations while maintaining consistency with LCA-based evaluation principles. More importantly, it facilitates large-scale exploration of material combinations, supports analysis of complex trade-offs between sustainability objectives and design constraints, and improves the identification of optimal or near-optimal solutions during the early design stage. Consequently, intelligent decision-support tools capable of systematically generating and evaluating diverse material scenarios within fixed design layouts are becoming increasingly important (Rizzo, 2025; Ashkbous et al., 2026).

It is important to distinguish between AI-predictive modelling and the DSF itself. Predictive models function primarily as surrogate evaluators of sustainability performance, estimating key indicators such as environmental burdens, recyclability, and cost (Dai et al., 2026). In contrast, the DSF represents a higher-level integrative architecture that combines scenario generation, predictive modelling, and optimisation into a unified computational framework for systematic exploration of the design space and identification of optimal or near-optimal solutions (Kebede et al., 2026). Within this context, predictive models constitute only one component of the broader decision-making process.

AI is introduced in this study not as a replacement for LCA, but as an enabling mechanism for embedding LCA within a scalable and optimisation-driven DSF. By serving as a computationally efficient surrogate model, AI enables rapid prediction of sustainability indicators across thousands of potential material combinations, thereby overcoming the computational limitations associated with repeated full-scale LCA evaluations. This integration enables continuous exploration of complex design spaces and supports efficient multi-objective optimisation under uncertainty. Such capability is particularly critical during early-stage design, where rapid and informed decision-making is essential despite incomplete information and competing sustainability priorities. Accordingly, the proposed framework should be interpreted as an optimisation-oriented decision-support system rather than a predictive replacement for LCA. While sensitivity-analysis methods can efficiently quantify the influence of individual parameters and assess uncertainty propagation within linear LCA models, they do not inherently provide mechanisms for systematic search, ranking, and optimisation of alternative material configurations under multiple sustainability objectives. These functions are performed within the present framework through the integration of predictive modelling and optimisation procedures.

To address these limitations, this study develops an AI-driven framework for systematic exploration and optimisation of construction material configurations within a fixed building design. The approach integrates LCA, scenario-based material substitution, predictive modelling, and optimisation to enable efficient evaluation across a large material design space. A reinforced-concrete case study demonstrates the framework's capability to identify environmentally efficient configurations while maintaining structural equivalence.

## 2. Method and materials

The methodological framework is general and independent of specific building types or datasets; however, it is demonstrated through a real-world case study. As illustrated in Fig. 1, the proposed framework operates as an integrated decision-support workflow comprising three interconnected stages. Stage 1 establishes the decision space by quantifying the benchmark material inventory, generating feasible material-substitution scenarios, defining sustainability-oriented performance criteria, and constructing the underlying data library. Stage 2 forms the predictive component of the framework, where the sustainability-based mixture-of-experts models are developed to capture the relationships between material configurations and sustainability performance indicators. Unlike AI-based predictive modelling, which is used to

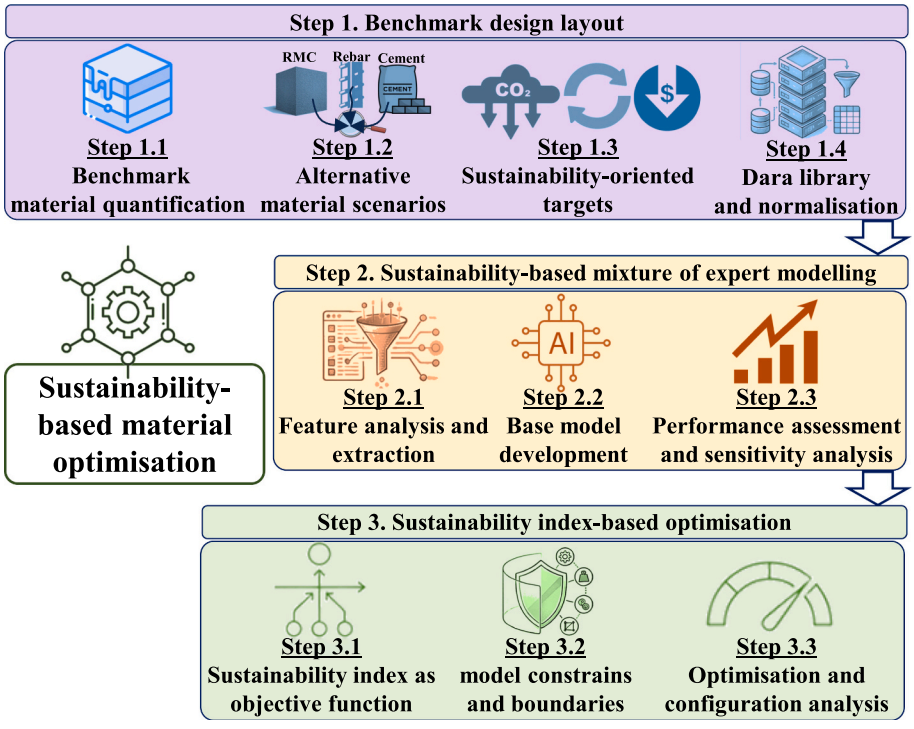


**Fig. 1.** Overview of the proposed framework for sustainable construction material optimisation.

estimate sustainability indicators for alternative material configurations, sensitivity analysis is employed to interpret model behaviour and quantify the influence of individual variables on the predicted outcomes. Building upon these validated predictive relationships, Stage 3 represents the decision-support component of the framework, where sustainability-index-based optimisation is used to systematically explore the feasible design space and identify optimal or near-optimal material configurations.

Accordingly, while sensitivity analysis is used to evaluate parameter influence and model behaviour, the AI-assisted optimisation framework enables systematic evaluation and ranking of alternative material configurations within the decision-support process. AI therefore serves as the predictive engine of the framework, sensitivity analysis provides model interpretability and validation, and optimisation translates the generated knowledge into actionable design decisions. The decision-support capability therefore emerges from the integration of scenario generation, sustainability assessment, predictive modelling, sensitivity analysis, and optimisation within a unified workflow.

The scope of the present study is limited to building-level material optimisation within a fixed reinforced-concrete office-building configuration and does not aim to perform a comprehensive urban-scale material-stock or built-form assessment. The primary objective of the research is to develop and validate an integrated AI-assisted LCA framework capable of systematically exploring and optimising alternative material configurations under controlled geometric and functional conditions. Accordingly, the benchmark building geometry, floor area, occupancy function, and structural system were intentionally maintained constant to isolate the influence of material-selection strategies, recycled content, and end-of-life pathways on sustainability performance. Consequently, broader urban-planning variables, including urban density, residential and commercial typologies, occupancy distribution, gross floor area per capita, and differences between urban, suburban, and rural built forms, were considered beyond the scope of the current investigation. Nevertheless, the proposed framework is designed as a scalable methodology and can be extended in future work toward multi-building and planning-scale applications to support comparative sustainability assessment across different urban-development and building-stock contexts.

### 2.1. Step 1: benchmark design layout

The benchmark model represents a business as usual (BaU) reinforced concrete office building located in the United Kingdom. As shown inf Fig. 2, the building comprises five storeys with total gross floor area is 2230 $m^2$, of which 1183 $m^2$ is habitable office space. The structural system consists of cast-in-place reinforced concrete moment-resisting frames with shear walls, supported by reinforced concrete foundations. Floor systems use two-way reinforced concrete slabs, consistent with typical UK mid-rise office construction. The benchmark reflects conventional design practice and standard material specifications, without incorporating circular design strategies, recycled-content optimisation, or alternative EoL pathways.

#### 2.1.1. Step 1.1: benchmark material quantification

Material quantities for the benchmark were derived from a detailed take-off based on architectural drawings, structural layouts, and reinforcement schedules. The take-off was performed at element level and subsequently aggregated into LCA categories. Reinforcement quantities were calculated from bar schedules and geometric measurements, covering foundations, columns, beams, slabs, shear walls, and stairs. Concrete volumes were determined for all structural elements and converted to material masses where required. Non-structural materials, including masonry blocks, mortars, renders, and finishes, were quantified from measured surface areas using standard material densities.

All LCA modelling calculations were performed directly within the OneClickLCA environment. LCA modelling was conducted using One-Click LCA, selected for compatibility with EN 15978 workflows, covering substructure, structure, enclosure, and primary finishing elements. Mechanical, electrical, plumbing, and fit-out systems were excluded to ensure consistency with early-stage embodied carbon assessment practice. The benchmark model includes substructure, superstructure, enclosure, and primary architectural elements. Mechanical, electrical, plumbing, HVAC systems, and secondary finishes were excluded. Therefore, environmental coefficients and inventory factors were not manually assigned but automatically retrieved from the selected EPDs (Listed in Table A4 in the Appendix A) and generic datasets associated with each material configuration. This workflow ensured methodological consistency, traceability, and comparability across all generated scenarios.

The environmental data used in this study were obtained through the OneClickLCA platform, primarily based on EPDs provided by manufacturers and available within the platform database. For scenarios where product-specific EPDs were not available, generic UK datasets integrated within the platform were adopted. These generic datasets represent country-specific average environmental profiles developed using aggregated EPD information together with bottom-up life-cycle

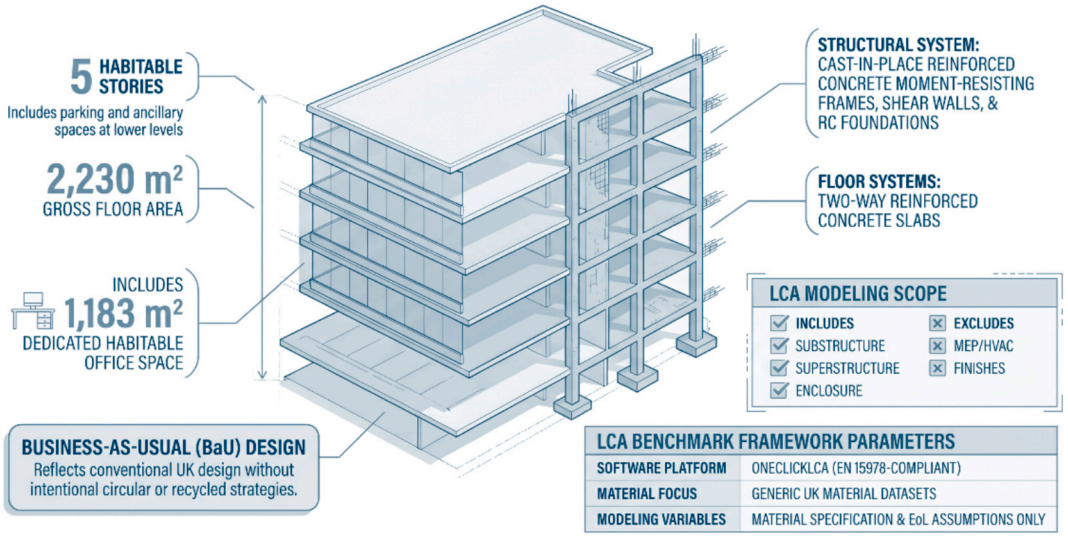


**Fig. 2.** Benchmark building specification for UK office baseline

inventory modelling approaches adapted to UK manufacturing conditions, transportation assumptions, energy mix, and end-of-life treatment pathways (Pasanen, 2025). The datasets were applied consistently across all scenarios to ensure comparability and alignment with EN 15804 and EN 15978-based life-cycle assessment practices.

Materials were modelled as virgin-dominant with default UK transport assumptions. No recycled content, reuse, or recovery credits were included. EoL scenarios followed standard disposal and landfill pathways, reflecting current industry practice. The benchmark establishes a fixed reference against which all alternative material scenarios are evaluated. In subsequent steps, geometry, building function, and baseline quantities remain unchanged. Variations in environmental performance therefore arise solely from differences in material specification and EoL assumptions.

The contribution of principal life-cycle stages to the environmental impact indicators of the benchmark building, obtained from the One-Click LCA model, is summarised in Table 1, with further details provided in Tables A1–A4 in the Appendix. As shown, the material stage (A1-A3) accounts for the largest share of the LCA indicators and is therefore selected as the primary target EC optimisation.

Table 2 presents material quantities of the BaU benchmark model used as the reference for all subsequent scenario analyses. Quantities are reported at material-category level to ensure a stable and transparent baseline while avoiding unnecessary product-level disaggregation. These quantities remain invariant across all scenarios; only material composition, recycled content, and EoL assumptions are modified in later steps.

The alternative scenario space is restricted to reinforcement steel (REB), structural ready-mix concrete (RMC), and Portland cement (CEM), as these dominate embodied environmental impacts in the benchmark model and govern system response under fixed geometry and function. The BaU LCA shows that REB, RMC, and CEM account for the majority of production-stage impacts (A1–A3), particularly for global warming, while other materials contribute comparatively minor shares despite, in some cases, large quantities. Within reinforced-concrete systems, these materials act as primary environmental control variables. Variations in composition or production route therefore produce system-level impacts significantly greater than those associated with non-structural materials. It should be mentioned here, although materials such as plasterboard, glass, aluminium, insulation, bitumen, plastics, paint, carpet, and copper were included within the baseline life-cycle inventory, they were not parameterised within the framework because their contribution to the total embodied impacts of the investigated reinforced-concrete structural system was comparatively smaller than that of reinforcement steel, concrete, and cement. Furthermore, maintaining these materials constant reduced unnecessary combinatorial complexity while preserving the dominant environmental drivers governing system-level performance.

This dominance arises from coupled process-level characteristics. Reinforcement steel exhibits high cradle-to-gate impact intensity due to energy- and carbon-intensive production routes. Portland cement is governed by clinker-related process emissions and high thermal energy demand. Structural concrete inherits this burden from its cementitious fraction, with binder composition controlling most embodied carbon. Benchmark results confirm this coupling, showing that variation in these streams produces first-order changes in life-cycle impacts, whereas non-structural materials induce only second-order effects without altering impact rankings.

**Table 2**
Benchmark material quantities defining the BaU reference model.

| Material category | Specification | Total quantity | GW (%) |
|---|---|---|---|
| REB_0: Reinforcement steel | Reinforcement steel (rebar), generic, 0% recycled content, A615 | 208,282 kg | 30.80 |
| RMC_0: Structural concrete (total) | Ready-mix concrete, normal strength, generic, C25/30 (3600/4400 PSI), with CEM I, 0% recycled binders (280 kg/m3 total cement) | 1643 $m^3$ | 41.32 |
| CEM_0: Portland cement (total) | Portland cement, generic, CEM I, 0% recycled binders | 489,282 kg | 7.08 |
| Sand and gravel (aggregates) | Aggregate (crushed gravel), generic, dry bulk density, 1600 kg/m3 | 3,284,718 kg | 4.63 |
| Chalk and gypsum-based materials | Gypsum plaster board, regular, 10% recycled gypsum, 6.5–25 mm, 10.725 kg/m2 (for 12.5 mm), 858 kg/m3 | 83,990 kg | 2.53 |
| Floor and wall finishes (tiles, stone, mosaic) and other materials | Ceramic glazed tile, 20 kg/$m^2$; Natural stone slab, flexible, indoor usage, 20 mm, 52 kg/$m^2$, 2600 kg/$m^3$, EN15804 + A1 | 5705 $m^2$ | 13.64 |

Scenario generation therefore targets binder substitution in concrete, recycled content and production-route variation in reinforcement steel, and clinker-reduced cement formulations. These parameters address dominant emission sources and represent the primary levers for modifying system-level performance while preserving structural equivalence and functional definition.

All remaining categories, including aggregates, autoclaved aerated concrete blocks, mortars, gypsum-based products, and finishes, are retained in the inventory but excluded from scenario parameterisation. Although some occur in large quantities, their cradle-to-gate emission factors are relatively low, and their contribution to total global warming remains minor. In particular, aggregate production contributes negligibly compared with the cement fraction in concrete. Including these materials would increase combinatorial complexity without meaningful impact variation. Restricting the scenario space to REB, RMC, and CEM therefore preserves the principal environmental drivers and enables focused comparison across technically relevant specifications.

The system boundary adopted in this study is defined as cradle-to-cradle. However, operational carbon emissions associated with modules B6-B7, together with other use-stage impacts related to modules B1-B5, were excluded from the analysis. This exclusion was considered

**Table 1**
Environmental impacts of BaU project.

| Stage cycle | Title | LCA parameter (%) | | | | | | |
|---|---|---|---|---|---|---|---|---|
| | | GW | AC | EU | PO | OD | AF | AN |
| A1-A3 | Construction Materials | 69.04 | 64.90 | 66.68 | 69.86 | 71.56 | 29.74 | 65.60 |
| A4 | Transport | 1.95 | 3.73 | 1.10 | 0.58 | 0.48 | 14.44 | 2.36 |
| A5 | Construction | 6.57 | 7.02 | 9.66 | 7.14 | 5.87 | 4.51 | 8.13 |
| B1-B3 | Operational | 5.43 | 5.10 | 5.24 | 5.49 | 5.63 | 2.34 | 5.16 |
| B4–5 | Replacement | 15.51 | 14.58 | 14.98 | 15.70 | 16.08 | 6.68 | 14.74 |
| C1-C4 | End of life | 1.50 | 4.66 | 2.33 | 1.22 | 0.37 | 42.29 | 4.02 |

AC: Acidification potential; AF: Fossil Abiotic depletion; AN: Non-fossil Abiotic depletion, EU: Eutrophication potential; GW: Global warming potential; OD: Ozone depletion potential; PO: Photochemical ozone formation

appropriate within the defined scope and system boundary of the present study because the primary objective was to isolate and quantify the influence of material-selection and end-of-life strategies on sustainability performance. To ensure a consistent basis for comparison, all non-material parameters, including building geometry, floor area, structural configuration, occupancy assumptions, operational conditions, building services, and service life, were maintained as fixed inputs across all investigated scenarios. Consequently, the environmental, economic, and circularity differences observed between scenarios arise exclusively from changes in material composition and end-of-life management pathways.

It is acknowledged that other factors, such as renewable energy systems, operational energy performance, maintenance strategies, user behaviour, and variations in building service life, can significantly influence whole-life sustainability performance. However, these parameters were intentionally excluded from the optimisation framework to avoid introducing additional sources of variability that could obscure the specific effects of material-related decisions. Therefore, the results should be interpreted as a comparative assessment of alternative material and end-of-life strategies under otherwise identical building conditions. Future research may extend the framework by incorporating operational energy systems, renewable technologies, maintenance interventions, and dynamic service-life scenarios to provide a more comprehensive whole-life optimisation approach.

#### 2.1.2. Step 1.2: alternative material scenarios

An alternative material scenario is defined as a unique combination of material specifications applied to a fixed benchmark geometry, with building function, layout, and element quantities unchanged. Substitutions are restricted to functionally equivalent options to preserve structural performance. Scenarios are generated by systematically varying (i) concrete mix composition, (ii) recycled content of reinforcement steel, (iii) cement specification, and (iv) EoL treatment for key material groups.

Tables A5 and A6 summarise the structure of the scenario space derived from the benchmark model. Scenarios are constructed through combinatorial assembly of discrete material options while preserving geometry and quantities. Alternatives are selected from verified datasets within OneClick LCA to ensure modelling consistency. From 124 RMC, 176 REB, and 47 CEM datasets, 8, 19, and 8 materials are selected, respectively, based on geographical feasibility and industrial relevance (UK/Ireland location, UK representation, or generic UK Environmental Product Declarations - EPDs).

For ready-mix concrete, scenarios vary mixes within the same strength class through partial substitution of Portland cement with supplementary cementitious materials (e.g., GGBS or fly ash) at predefined ratios. For reinforcement steel, scenarios vary recycled content and production routes, from virgin-dominant to high secondary content. For cement, scenarios incorporate clinker reduction and alternative EoL recovery options. Modifications are applied individually and in combination, enabling assessment of isolated effects and interaction responses.

Although the scenario library was generated through systematic combinatorial material substitutions, the resulting dataset does not represent unconstrained synthetic data generation. All scenarios were derived from a real-world reinforced-concrete office-building benchmark model using actual material quantities obtained from detailed inventory take-offs. Furthermore, all alternative material specifications and end-of-life pathways were selected exclusively from manufacturer-specific Environmental Product Declarations (EPDs) and geographically relevant UK-based datasets available within the One Click LCA platform. The generated scenarios were additionally constrained by structural equivalence, practical constructability, material availability, and realistic industry conditions to ensure technical feasibility and real-world applicability.

This structured approach generates over 1500 technically feasible scenarios for early-stage evaluation. Material quantities remain invariant across all models to ensure comparability. Variations in performance therefore arise solely from differences in material specification and EoL treatment, consistent with early-stage LCA practice and enabling direct scenario comparison. All scenarios are constrained by material availability, design feasibility, and dataset boundaries, ensuring that the generated combinations remain representative of realistic construction conditions rather than unconstrained synthetic data.

#### 2.1.3. Step 1.3: sustainability-oriented targets

Sustainability performance is evaluated using three target families (Table 3). The first captures environmental impacts derived from life-cycle inventory results in OneClick LCA. The second quantifies circularity performance under scenario-specific product-stage and EoL routing. The third represents a monetary proxy for socio-economic burden through LC outputs, where available.

Environmental performance was characterised using six midpoint indicators derived from the LCA defined in ISO 14040 (ISO, 2015), ISO 14044 (ISO, 2006), EN 15804 (BSI, 2019) and EN 15978 (BSI, 2012). These indicators were selected to represent three key environmental dimensions relevant to sustainable building design: Embodied carbon (EC) is included because climate-change mitigation is the dominant sustainability objective in contemporary building design and is widely recognised as the primary environmental performance indicator in the construction sector (Cabeza et al., 2014; Ahmadi et al., 2025). Ozone depletion (OD), AC, and EU), are selected to capture atmospheric and ecosystem impacts arising from material production and EoL processes (Kirchherr et al., 2017). Abiotic depletion of elements (AN) and fossil resources (AF) are included to assess resource consumption and long-term resource scarcity, which are central considerations in circular-economy and material-efficiency assessments (Geissdoerfer et al., 2017). Together, these six indicators provide coverage of climate impacts, ecosystem impacts, and resource-depletion impacts while

**Table 3**
Sustainability-oriented targets used for scenario evaluation.

| Indicator | ID | Unit | Description | Sensitivity to EoL definition |
|---|---|---|---|---|
| Embodied carboSOn | EC | kg $CO_{2e}$ | Embodied climate-change impact across life-cycle stages | High; affected by recycling, recovery, and disposal routes |
| Acidification potential | AC | kg $SO_{2e}$ | Emissions contributing to acidification of soils and water bodies | Moderate; influenced by processing and transport at end of life |
| Eutrophication potential | EU | kg $PO_{4e}^{3-}$ | Nutrient-related impacts on aquatic and terrestrial ecosystems | Moderate; sensitive to waste-processing emissions |
| Ozone depletion potential | OD | kg CFC11 | Depletion of stratospheric ozone | Indirectly influenced by upstream and EoL processes |
| Fossil Abiotic depletion | AF | MJ | Consumption of fossil energy resources | High; linked to energy intensity of production and recovery |
| Non-fossil Abiotic depletion | AN | kg $Sb_e^-$ | Depletion of mineral and metal resources | Reduced by higher recycled content and effective recovery |
| Circularity | CE | % | Degree of circular material inflow and outflow | Directly controlled by EoL routing |
| Life-cycle cost | LC | £K | Comparative monetary burden over the life cycle | Influenced by disposal and recovery pathways where cost data exist |

avoiding excessive redundancy between highly correlated environmental indicators. Their selection therefore enables a balanced evaluation of environmental sustainability while maintaining computational efficiency and interpretability within the optimisation framework. However, photochemical ozone formation is excluded due to negligible variation across scenarios. Global warming is not retained separately, as EC represents the climate-change impact of embodied life-cycle stages; including both would introduce redundancy. EC is therefore adopted as the representative climate metric.

The second target family quantifies circularity using building-level metrics generated within the modelling platform (inspired by Ahmadi et al., 2024, 2025). It captures upstream characteristics, including recycled content and binder substitution (e.g., GGBS or fly ash), and downstream EoL routing such as recycling, reuse, backfilling, or disposal. Circularity thus reflects scenario-specific EoL definitions and complements impact-based environmental indicators.

The third target family represents a monetary proxy for socio-economic implications (LC), expressed through discounted outputs recommended by EN 15978 and EN 15804 (BSI, 2012, 2019). Results are reported consistently across all scenarios using cost-related outputs within OneClick LCA. Values are interpreted comparatively rather than as absolute estimates, reflecting the generic nature of the datasets and their role as indicators of relative socio-economic burden rather than project-specific costs.

#### 2.1.4. Step 1.4: data library and normalisation

A centralised digital data library was established to support modelling and optimisation. Scenario outputs were compiled into a structured matrix, where each row represents a material configuration and each column a quantitative sustainability variable or encoded design descriptor. Environmental, circularity, and life-cycle indicators were stored in numerical form and linked to scenario identifiers through a consistent coding structure. Categorical variables for material specifications and EoL pathways were encoded into machine-readable formats, with a reference key maintained to preserve traceability. The dataset was stored in interoperable tabular formats to ensure compatibility with statistical analysis and supervised learning.

To ensure comparability across heterogeneous indicators, a dimensionless normalisation framework was applied, following Ahmadi et al. (2025). All outputs were scaled relative to a fixed reference, as defined in Eq. (1), expressing performance as proportional deviation from the baseline. This removes unit inconsistency (e.g., kg $CO_2$e, MJ, kg Sb-eq, £k) and harmonises magnitude differences that could bias learning algorithms. Burden indicators were scaled such that reductions yield values below unity, while benefit indicators were transformed to maintain a consistent minimisation orientation. This unified structure enables coherent integration within multi-objective modelling and index formulation.

$$ST_{i,j} = \begin{cases} \dfrac{RST_{i,BaU}}{RST_{i,j}} \text{ if higher } RST_{i,j} \text{ indicates better sustaniaiblity} \\ \dfrac{RST_{i,j}}{RST_{i,BaU}} \text{ if higher } RST_{i,j} \text{ indicates lower sustaniaiblity} \end{cases} \quad (1)$$

where $St_{i,j}$ denotes the normalised value of the $i^{th}$ sustainability-oriented target (e.g., EC or CE) for scenario j (i.e material's alternative scenario under evaluation), and RST denotes the raw value of the sustainability-oriented target.

#### 2.1.5. Step 2: sustainability-based mixture of expert modelling

To ensure computational efficiency during optimisation, a back-propagation neural network (BPNN) was adopted for predictive modelling developed and trained using MATLAB R2023a. The initial configuration used 38 input variables (8 RMC, 19 REB, 8 CEM, and 3 EoL options) to predict eight outputs. This formulation was subsequently revised. First, when the architecture was evaluated using the capacity sanity-check approach recommended by Vandersmissen and Oramas (2024) and Hu et al. (2025), the samples-per-parameter ratio was approximately 3.9 (see Part B in Appendix for full calculation). Although not indicative of overfitting, this falls within a moderate regime where generalisation is uncertain, limiting statistical robustness under the bias–variance trade-off. Second, most parameters were concentrated in the first hidden layer (38 × hidden neurons), meaning model capacity was governed primarily by input dimensionality. This increases susceptibility to spurious correlations, particularly under multicollinearity among inputs (Lighittha et al., 2026; Peng et al., 2026). Third, the multi-output structure increases task complexity and may reduce model stability. Reducing input dimensionality or restructuring the input–output formulation improves interpretability and reduces sensitivity to random initialisation and data partitioning (Kang et al., 2026).

#### 2.1.6. Step 2.1: feature analysis and extraction

To reduce input dimensionality, clustering analysis was applied using Gaussian mixture models (GMM), hierarchical agglomerative clustering (dendrogram analysis), t-SNE, and PCA projections of GMM clusters (Appendix C). Results show that input variables can be reduced while preserving the underlying data structure. Accordingly, the high-dimensional input space was restructured by aggregating detailed material variables into composite array-based descriptors. Instead of using multiple individual inputs for CEM, REB, and RMC, each material family was encoded as a single structured array capturing its internal composition. This transformation reduces effective dimensionality while preserving intrinsic relationships among components. By compressing correlated features into unified representations, the number of trainable parameters—particularly in the first hidden layer—was significantly reduced, improving model stability and generalisation.

#### 2.1.7. Step 2.2: base model development

The BPNN architecture comprises three hidden layers, each with five neurons (as shown in Fig. 3. This compact configuration balances model flexibility and generalisation capacity, avoiding over-parameterisation relative to the available dataset size (Piadeh et al., 2023; Bibri and Huang, 2025). To further control model complexity and enhance flexibility, a modular strategy based on the mixture-of-experts framework (Li and Sung, 2025; Xi et al., 2025) was adopted. Instead of a single multi-output network, separate models were trained for each target variable. Each model is stored in a library and operates as an independent expert.

#### 2.1.8. Step 2.3: performance assessment and sensitivity analysis

The performance of the expert models was evaluated using **Root Mean Square Error (RMSE)** and the **coefficient of determination ($R^2$)** under previously unseen **single-variation scenarios**. However, this evaluation alone is insufficient to demonstrate the true predictive capability of the developed models, as these cases still represent interpolations within the original scenario space. To address this limitation, an additional **40 scenarios** were constructed incorporating different combinations of all considered material groups. These multivariate scenarios are entirely new and differ substantially from the structure of the training data, thereby providing a more rigorous assessment of the models' generalisation capability.

Beyond RMSE and $R^2$, **model bias** was also examined to provide a more comprehensive evaluation. Specifically, **underestimation bias, overestimation bias, and aggregate emission bias** were quantified to assess systematic prediction errors and to verify that the models do not consistently under- or over-predict emissions across different material configurations.

In addition to the quantitative performance metrics, three explainable artificial intelligence (XAI) analyses were conducted to ensure the transparency, reliability, and robustness of the developed models. These included **Layer-wise Relevance Propagation (LRP)** to identify the contribution of input features to model predictions, **Shapley Additive Explanations (SHAP)** analysis to quantify and interpret feature

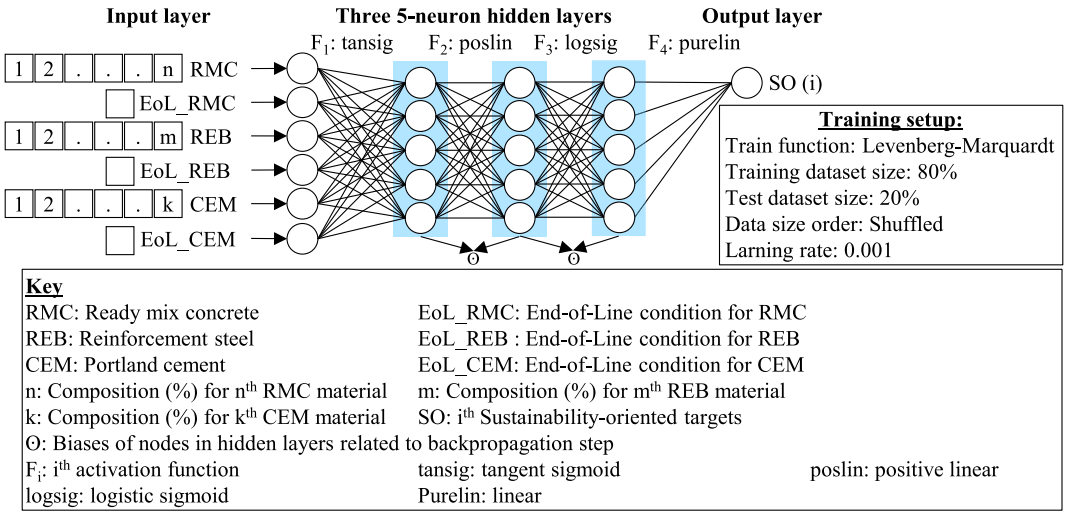


**Fig. 3.** Structure of the mixture of expert models developed

importance across scenarios, and systematic **underfitting and overfitting checks** using the 40 newly constructed multivariate scenarios.

*2.1.9. Step 3: sustainability index-based optimisation*

Unlike the predictive modelling phase, where scenarios were generated through controlled substitutions with one material varied at a time, the optimisation framework enables simultaneous adjustment of multiple material shares. The model is therefore not restricted to predefined substitution pathways and can generate new material combinations within defined feasibility bounds. This facilitates exploration of more diverse and complex mixtures not explicitly represented in the training dataset. The optimisation stage addresses a fundamentally different problem from conventional sensitivity analysis. Sensitivity-analysis techniques evaluate how variations in predefined input parameters influence model outputs, whereas optimisation seeks to identify material configurations that best satisfy specified sustainability objectives while respecting practical design constraints. The role of the AI-based surrogate models is therefore to enable rapid evaluation of candidate solutions during the search process, allowing efficient exploration of a large feasible solution space that would otherwise require repeated execution of full LCA simulations.

Among the evaluated optimisation techniques, the shuffled frog leaping algorithm (SFLA) was selected here as shown in Fig. 4. This is mainly because, compared with commonly used optimisation approaches such as response surface methodology (Dewi et al., 2025), multi-objective optimisation (Sandanayake et al., 2022), and genetic algorithm or NSGA-II (Galimshina et al., 2022), SFLA provides a favourable balance between exploration and exploitation through cooperative information exchange between subgroups, enabling effective exploration of complex solution spaces while maintaining convergence stability (Piadeh et al., 2024). This characteristic is particularly advantageous for optimisation problems involving multiple interacting design variables, nonlinear predictive models, and high-dimensional sustainability trade-offs (Offie et al., 2023), as considered in this

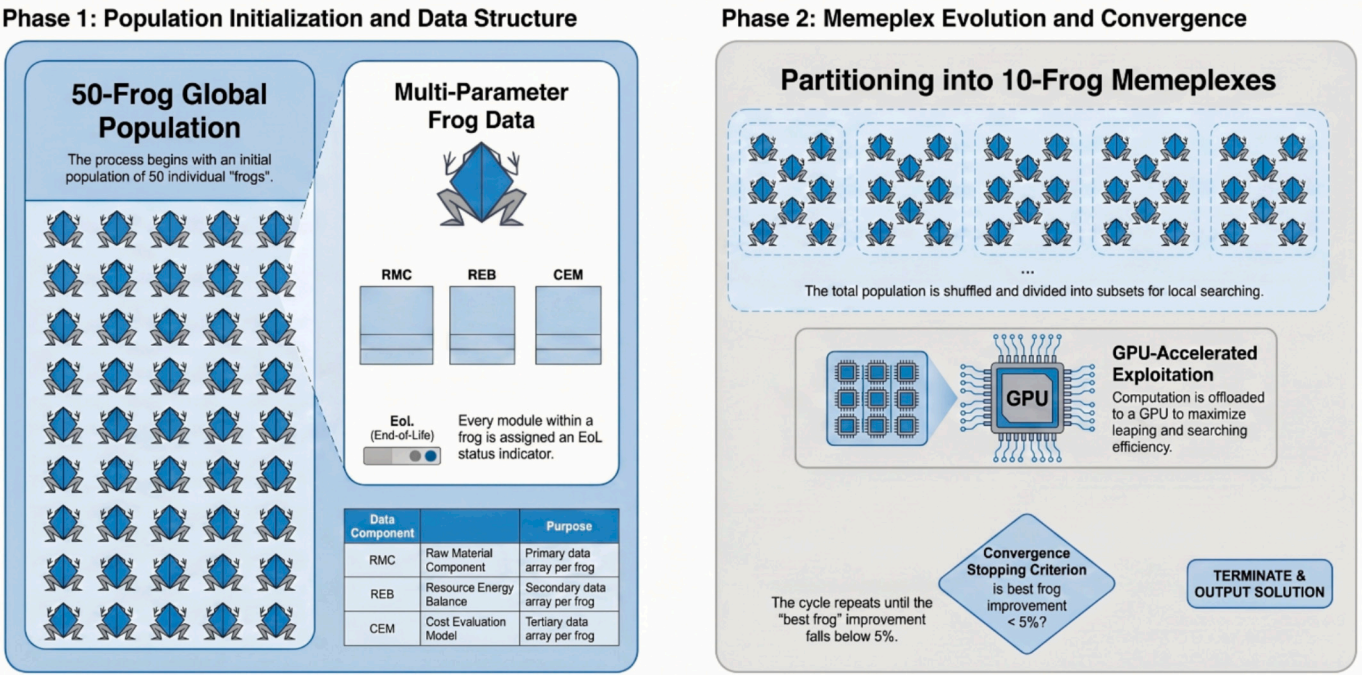


**Fig. 4.** Workflow of the Shuffled Frog Leaping Optimisation Algorithm used in this study

study. Furthermore, SFLA exhibits relatively low parameter sensitivity and computational demand compared with several evolutionary optimisation approaches, enhancing its suitability for iterative optimisation processes integrated with AI-based predictive frameworks (Chamlal et al., 2024). The combination of convergence stability, computational efficiency, and robustness under complex nonlinear conditions therefore motivated the selection of SFLA as the optimisation engine for the proposed framework (Azghandi et al., 2025).

#### 2.1.10. Step 3.1: sustainability index as objective function

The primary objective function adopted in the optimisation framework is the **SI**, conceptually inspired by Carreira-Barral et al. (2026). However, the original formulation has been extended and refined, as presented in Eq. (2), to better accommodate the structure of the predictive modelling framework and the multi-criteria nature of the design problem. The purpose of the SI is to integrate multiple performance criteria, according to the **decision-maker's strategic preferences**, into a single scalar objective function that enables systematic comparison and optimisation of material design scenarios.

The formulation allows the relative importance and inclusion or exclusion of each target variable to be controlled through an adjustable weighting factor $W_i$. By modifying these weights, the optimisation framework can represent different sustainability priorities without altering the underlying predictive models. This adaptable weighting structure ensures that the optimisation process remains flexible and transparent, while maintaining a unified and mathematically consistent decision-making framework aligned with varying policy, environmental, or economic objectives.

$$SI = \frac{\sum_{i=\text{number of targets}} W_i \times ST_i}{\sum_{i=\text{number of targets}} W_i} \quad (2)$$

where $W_i$ is the importance weight assigned to the $i^{th}$ sustainability-oriented target, $ST_i$ denotes the normalised value of the $i^{th}$ sustainability-oriented target.

The weighting factors can be interpreted as direct inputs from stakeholders or decision-makers, allowing the framework to reflect different strategic priorities. By adjusting these weights, users can emphasise environmental performance, circularity, or economic considerations without modifying the underlying predictive models. This enables the framework to function as a flexible decision-support tool tailored to varying design objectives and policy requirements.

#### 2.1.11. Step 3.2: model constrains and boundaries

The decision variables representing material shares for RMC, REB, and CEM were formulated as compositional variables and were therefore subject to strict mixture constraints. Each share variable was bounded within the interval [0%, 100%], and the total contribution within each material group was constrained to sum exactly to 100% (i.e. $\sum(i{:}1 \rightarrow 9)\ REM_i = 100$; $\sum(i{:}1 \rightarrow 20)\ REB_i = 100$; $\sum(i{:}1 \rightarrow 9)\ CEM_i = 100$), thereby preserving physical consistency and mass balance within the mixture formulation.

To reflect practical blending, procurement, and supply-chain considerations, a sparsity constraint was imposed on the number of simultaneously active components in each material group. Specifically, no less than 1 and no more than "n" components per group (i.e.$1 \leq$ Nnz (group materials) $\leq$ n) were permitted to have non-zero contribution. This parameter can be adjusted according to the decision-maker's preferences, thereby controlling the structural complexity of the resulting mixture configurations.

To prevent the selection of unrealistically small material fractions, a minimum activity threshold was introduced, and quantities were rounded according to practical construction constraints. For RMC and CEM, thresholds were defined based on standard material supply units, with quantities rounded up to the nearest whole unit to avoid fractional material usage. For REB, the threshold was determined based on standard bar lengths, with quantities rounded up to the nearest whole bar to ensure constructability. This requirement ensures that each active component contributes a practically meaningful amount to the mixture and prevents the optimisation algorithm from exploiting extremely small fractional allocations. The EoL variables were treated as discrete categorical parameters and constrained to integer values. Following each optimisation update, a feasibility-repair mechanism was applied to ensure compliance with all compositional and discrete constraints. This procedure retained only the *m*largest share components within each material group and subsequently renormalised them to satisfy the 100% mixture constraint. The parameter *m*can be specified according to the designer's preferred level of mixture sparsity, providing flexibility in controlling the diversity and practicality of optimised material configurations. These constraints can be adjusted to reflect stakeholder preferences, procurement strategies, and practical implementation requirements, thereby linking the optimisation process to real-world decision-making conditions.

#### 2.1.12. Step 3.3: sustainability optimisation outcomes and material configuration analysis

To examine the behaviour of the optimisation framework under different sustainability priorities, five weighting strategies were defined for the SI. These scenarios were developed collaboratively through a focus-group workshop, implemented based on the recommendations of Piadeh et al. (2020) and involving 15 stakeholders selected from local authorities, industry, and academia. The validation and selection of stakeholders were also conducted in accordance with the recommendations of Parece et al. (2025a, 2025b). The characteristics of the selected stakeholders are provided in Table A7 in Appendix A.

In A1, EC was prioritised by assigning it a weight of 0.65, while the remaining criteria were each assigned a weight of 0.05. The same weighting structure was adopted in A2 and A3, where CE and LC were prioritised respectively. The use of a dominant weight of 0.65 ensures that the selected indicator strongly influences the optimisation objective, whereas assigning equal minor weights (0.05) to the remaining indicators retains their influence while preventing them from dominating the optimisation process. This weighting structure therefore allows the evaluation of optimisation behaviour when one sustainability objective is intentionally emphasised while the remaining criteria are still considered.

To examine balanced sustainability priorities, A4 assigns dominant weights of 0.25 to EC, circularity (CE), and LC, while remaining indicators receive 0.05 each. This configuration prioritises environmental impact, circularity, and economic performance while retaining secondary environmental effects. A5 defines a neutral case, assigning equal weights of 0.125 to all eight indicators, allowing optimisation without predefined preference.

For practical interpretation, solutions are restricted to a maximum of three active material options per group. This avoids highly fragmented mixtures that are impractical for procurement and construction. The constraint improves interpretability and aligns results with typical industry sourcing practices. For each strategy, the three best-performing solutions are retained and analysed to identify consistent patterns in material configurations.

To verify the reliability of the optimisation results, the optimal material combinations predicted by the AI-based framework were re-evaluated using OneClickLCA. This step enabled direct comparison between predicted sustainability indicators and values obtained from the original life-cycle assessment model. Agreement between predicted and observed results was assessed using normalised root mean square error (NRMSE) and normalised residual error, providing an independent validation of the predictive–optimisation workflow.

## 3. Results and discussion

### 3.1. Performance assessment of prediction models

Fig. 5 compares predicted and observed values for all eight

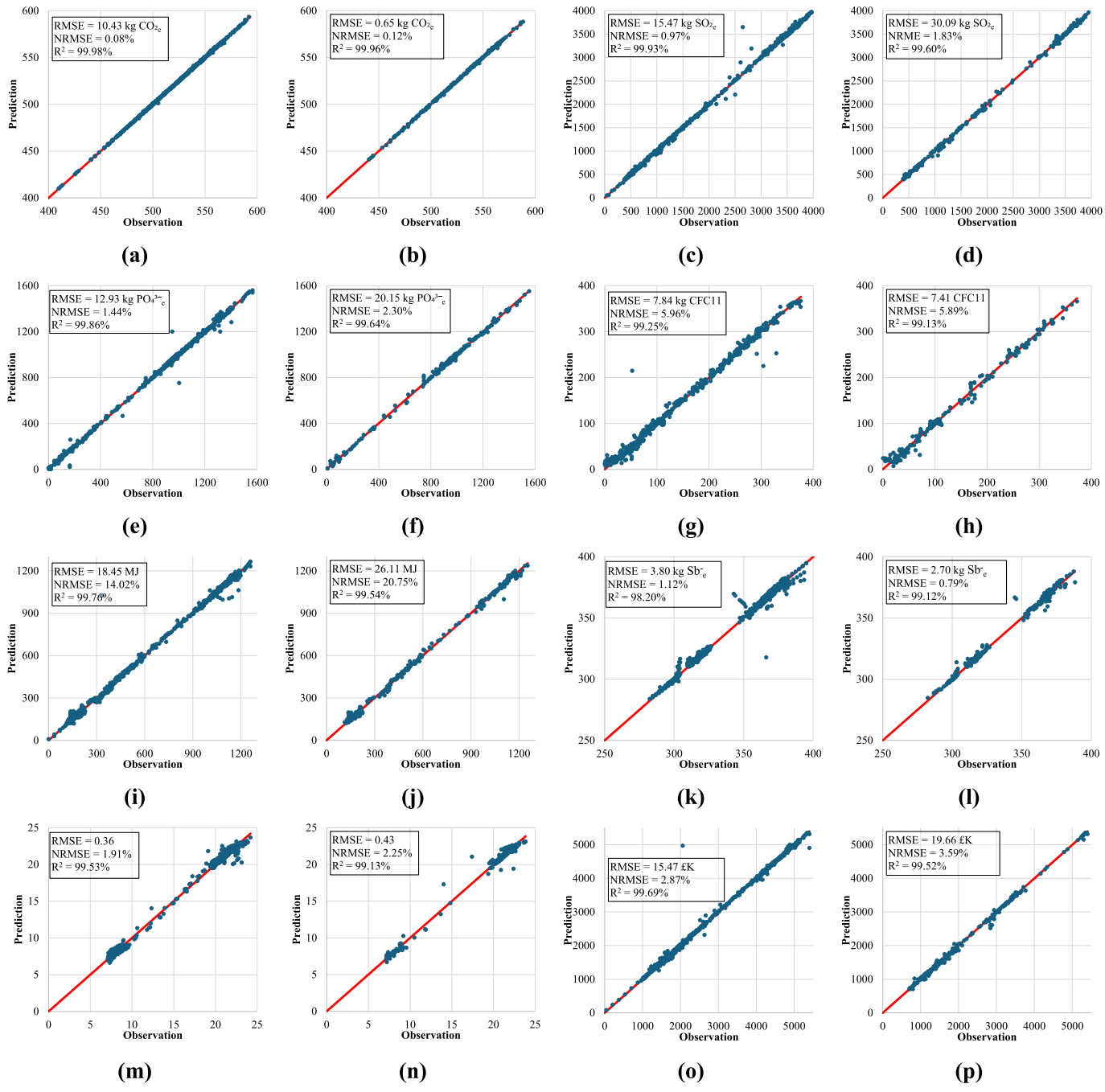


**Fig. 5.** Performance assessment of expert-based model developed on single variate scenarios: (a) EC train, (b) EC test, (c) AC train, (d) AC test, (e) EU train, (f) EU test, (g) OD train, (h) OD test, (i) AF train, (j) AF test, (k) AN train, (l) AN test, (m) CE train, (n) CE test, (o) LC train, (p) LC test.

sustainability indicators. Across all cases, the scatter points align closely with the 1:1 reference line, indicating strong agreement between the model predictions and the values obtained from the OneClick LCA simulations. The coefficients of determination remain consistently high for both training and testing datasets, ranging approximately from 98.20% to 99.98%, while the normalised prediction errors remain generally low. These results indicate that the developed models successfully reproduce the response of the original LCA simulations under single-factor variation.

The highest predictive accuracy is observed for EC, AC, and LC. For EC, the models achieve $R^2$ values of 99.98% and 99.96% for training and testing, respectively, with NRMSE values of only 0.08% and 0.12%, indicating an almost exact reconstruction of the simulated response. AC and LC show similarly strong performance, with $R^2$ values exceedingly approximately 99.5% and prediction errors remaining below about 1.9%. These indicators are largely governed by dominant material parameters, which leads to relatively smooth response relationships that can be learned efficiently by the predictive framework. Slightly larger deviations appear for indicators such as EU and CE, where testing errors increase moderately compared with training results, with NRMSE values reaching around 2–3% while maintaining $R^2$ values above 99%. Greater dispersion is observed for OD and AN, where $R^2$ values decrease slightly to approximately 99.25% and 98.20% and the NRMSE approaches about 5–6% in some cases.

The results demonstrate that the developed models accurately reproduce the response of the single-variation scenario space. However, these cases still represent interpolation within the original design domain. A more rigorous assessment of model robustness therefore

requires evaluation under multivariate conditions, which is presented in Fig. 6 using newly generated combinations of material variables.

Fig. 6 provides a rigorous and independent validation of the predictive framework, as the developed models were evaluated using 40 newly constructed multivariate scenarios with completely unseen material compositions that were not represented in the original training dataset. These additional scenarios were intentionally generated to assess the robustness, stability, and generalisation capability of the models under new combinations of input variables, thereby reducing the likelihood that the reported high prediction accuracy is associated with overfitting. Overall, the agreement between predicted and observed values remains strong for all indicators, with $R^2$ ranging from 96.5% to 99.24%. The best overall fit is obtained for AC and LC, with $R^2$ values of 99.24% and 99.11%, respectively, while CE, EU, and OD also remain highly accurate with $R^2$ values above 98.4%. Even EC, which shows the lowest $R^2 = 96.5\%$, still achieves confirming that the developed models retain strong predictive capability under simultaneous variation of multiple material groups.

The error metrics further confirm this robustness, although the indicators do not perform identically. AF shows the lowest relative error, with NRMSE = 1.25%, followed by EC (2.42%) and LC (3.72%), indicating particularly stable prediction of these responses. CE, AC, and EU remain within a moderate error band of about 4.5–5.0%, while OD reaches 5.93%. The largest relative deviation occurs for AN, where NRMSE increases to 10.65% despite $R^2$ remaining high at 98.37%. This combination suggests that the model captures the overall trend of AN well but exhibits larger local deviations for some multivariate cases. From a modelling perspective, this is reasonable, as AN is more likely to respond to distributed upstream inventory effects rather than to a single dominant material driver.

The bias terms show that systematic error remains limited for most indicators. For EC, EU, and AF, NBiasT is effectively zero, indicating that overestimation and underestimation are well balanced. LC also shows a very small total bias (0.37%), while CE exhibits a slightly larger positive total bias (0.81%), suggesting mild net overprediction. AC and OD show small negative total bias values (−0.61% and − 0.06%), indicating negligible net underprediction. The clearest directional bias appears for AN, where NBias− = 10.40% and NBiasT = −7.54%, showing that the model tends to underestimate this indicator more frequently or more strongly than it overestimates it. Nevertheless, the overall alignment of the data around the 1:1 line confirms that this effect is limited to a small number of cases and does not compromise the general predictive reliability of the framework.

This multivariate validation is a key strength of the study. Unlike the single-variation tests, these scenarios assess whether the models can predict sustainability responses for genuinely new combinations of material variables. The consistently high $R^2$ values, moderate NRMSE values for most indicators, and generally low signed bias confirm that the expert-based framework generalises well beyond the original scenario set and can be used with confidence in the subsequent optimisation stage.

The exceptionally high prediction accuracy achieved by the developed models can be partially attributed to the underlying characteristics of life-cycle assessment calculations. Several environmental indicators, particularly EC and life-cycle cost LC, are derived from inventory-based calculations in which environmental burdens are directly linked to material quantities through predefined characterisation factors. Consequently, these indicators tend to exhibit relatively smooth and deterministic response surfaces, which inherently enhance predictability compared with many engineering problems governed by complex physical phenomena and stochastic behaviour.

Nevertheless, the prediction task remains considerably more complex than a simple linear mapping between material quantities and sustainability outcomes. The developed dataset incorporates multiple material alternatives, discrete substitution strategies, and alternative end-of-life pathways, resulting in a large combinatorial solution space. Furthermore, different sustainability indicators are governed by distinct mechanisms. For example, EC and LC are primarily influenced by material inventories, whereas circularity performance CE is strongly affected by recovery, reuse, and recycling routes at the EoL. This behaviour is reflected in the SHAP analyses, which demonstrate substantial differences in feature importance across the sustainability indicators. The varying influence patterns suggest that the predictive framework captures indicator-specific relationships and interactions rather than merely reproducing a single deterministic trend. Therefore, while the structured nature of LCA calculations contributes to the high prediction accuracy, the results also demonstrate the capability of the proposed AI framework to learn complex interactions among material

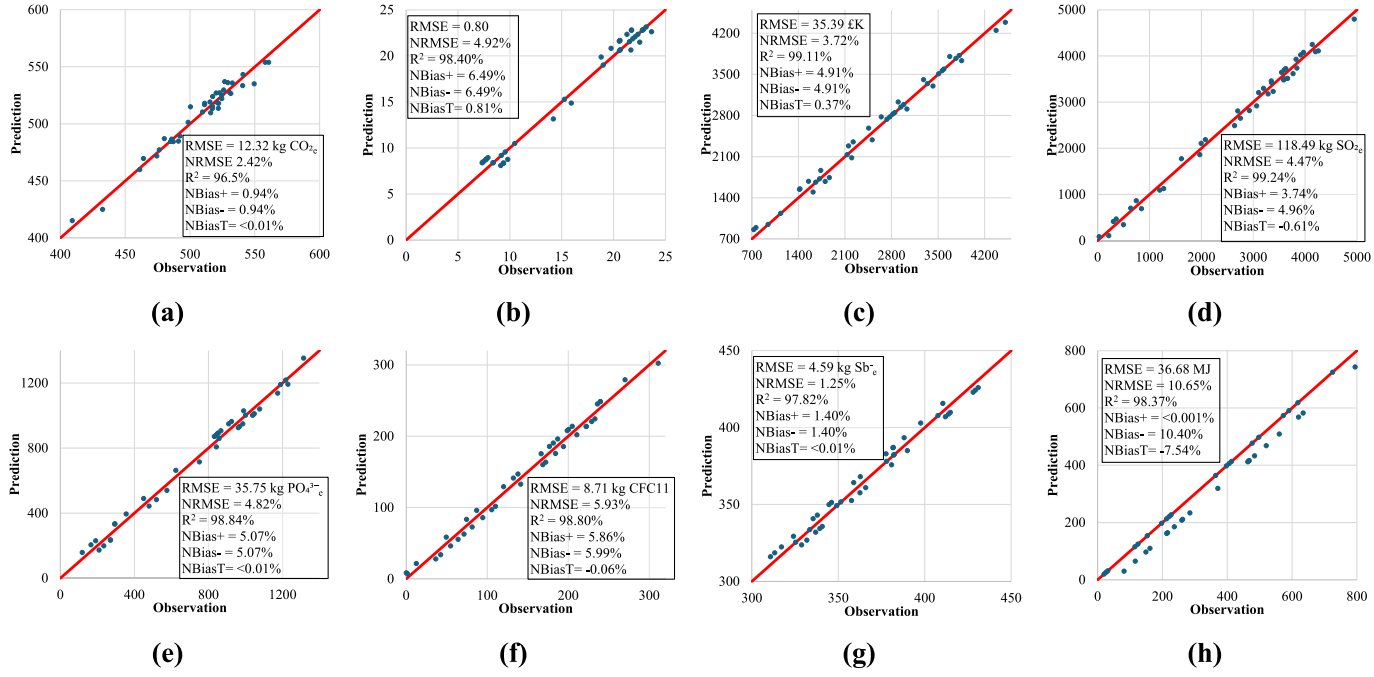


**Fig. 6.** Performance assessment on multi variate scenarios: (a) EC, (b) CE, (c) LC, (d) AC, (e) EU, (f) OD, (g) AN, (h) AF.

selection, end-of-life management strategies, and multiple sustainability objectives.

### 3.2. Sensitivity analysis of predictive models

The analysis focuses on EC, CE, and LC, which represent the most widely used sustainability indicators in both research and industrial decision-making, while the remaining indicators are provided in the Figs. A5–6 in the Appendix. Fig. 7(a) presents the uncertainty behaviour of the models as the proportion of training data decreases. Three stages can be observed. With large training datasets, prediction error remains very low, indicating strong resistance to overfitting. As the available data decreases, the model adapts while maintaining relatively stable accuracy. When the training data becomes significantly limited, prediction error increases more rapidly. The similar behaviour observed for EC, CE, and LC indicates that the predictive architecture maintains stable learning characteristics under varying data availability.

The influence of individual input variables is illustrated by the LRP diagrams shown in Figs. 5(b), 5(d), and 5(f). In these graphs, the thickness of the connections represents the relative contribution of each variable to the prediction. The bold links therefore indicate the dominant information pathways learned by the network. For EC and LC, the strongest connections originate from RMC and REB, indicating that concrete composition and reinforcement steel content are the primary drivers of embodied impacts and LC. In contrast, CE shows stronger links associated with EoL variables, reflecting the greater importance of recovery and recycling pathways in determining circularity performance.

The SHAP analyses presented in Figs. 5(c), 5(e), and 5(g) provide quantitative insight into the mechanisms governing each sustainability indicator. For EC, the largest SHAP distributions are associated with RMC and REB, indicating that variations in these materials exert the greatest influence on total carbon emissions. This behaviour is expected because concrete and reinforcement constitute the majority of the structural mass and are also among the most carbon-intensive materials within the life-cycle inventory. Consequently, marginal reductions in cement content, substitution with supplementary cementitious materials, or optimisation of reinforcement quantities are likely to produce substantially greater carbon savings than modifications to secondary material groups. A similar pattern is observed for LC, where RMC and REB again dominate the SHAP rankings. The consistency between EC and LC suggests a strong coupling between environmental and economic performance. In practical terms, strategies aimed at reducing concrete and reinforcement demand may simultaneously reduce both embodied carbon and project cost, indicating the presence of potential co-benefits rather than trade-offs. This finding is particularly important for early-stage design, where decisions regarding structural materials can influence both sustainability and budget performance.

In contrast, the CE exhibits a fundamentally different behaviour. The dominant SHAP values are associated with EoL routing variables, while most material-selection variables exhibit relatively limited influence. This suggests that circularity performance is governed less by the quantity of materials used and more by what happens to those materials after the building reaches the end of its service life. Therefore, improving circularity requires interventions such as increasing recycling rates, enhancing material recovery pathways, and designing for future disassembly and reuse, rather than simply reducing material consumption.

The differing SHAP patterns also reveal an important sustainability trade-off. Variables that strongly influence EC and LC are not necessarily the same variables controlling CE. As a result, a solution optimised solely for carbon reduction may not achieve the highest circularity performance, and vice versa. This observation justifies the multi-objective optimisation framework adopted in this study, as single-objective optimisation would fail to capture the competing influences of material selection and end-of-life management strategies.

Furthermore, the narrow SHAP distributions observed for several material variables indicate that their influence remains consistently low across the analysed scenarios. From a practical decision-making perspective, these variables may be considered lower-priority design parameters, allowing stakeholders to focus resources and optimisation efforts on the relatively small number of variables that drive the majority of sustainability outcomes. This provides a transparent basis for prioritising design interventions and supports more efficient allocation of engineering effort during early-stage sustainable building design.

Complexity in prediction task also is reflected in the SHAP analyses, which demonstrate substantial differences in feature importance across the sustainability indicators. The varying influence patterns suggest that the predictive framework captures indicator-specific relationships and interactions rather than merely reproducing a single deterministic trend. Therefore, while the structured nature of LCA calculations contributes to the high prediction accuracy, the results also demonstrate the capability of the proposed AI framework to learn complex interactions among material selection, end-of-life management strategies, and multiple sustainability objectives.

The interpretability analyses also provide practical insight for decision-makers and designers. By identifying the dominant variables influencing each sustainability indicator, the SHAP and LRP results enable stakeholders to better understand which material groups and EoL pathways govern environmental, circularity, and economic performance. This improves transparency of the optimisation process and supports more informed material-selection strategies by highlighting where modifications in material composition are likely to produce the greatest sustainability benefits. Furthermore, the consistency between the explainability analyses and the underlying physical behaviour of the material system increases confidence in the reliability and practical applicability of the proposed AI-driven framework. The consistency between LRP and SHAP results confirms that the predictive models capture physically meaningful relationships between material composition, EoL pathways, and sustainability indicators. This interpretability also provides confidence that the optimisation framework developed in the next section operates on realistic and well-structured input–output relationships, thereby supporting reliable identification of optimal material configurations.

### 3.3. Performance evaluation of optimisation model

Fig. 8 confirms that weighting structure governs both SI magnitude and solution behaviour. Circularity-focused optimisation (A2) achieves the lowest SI, indicating that targeting CE is most effective within the explored design space. Balanced strategies (A4-A5) produce similarly competitive results, whereas single-objective emphasis on EC or LC (A1, A3) leads to higher SI, reflecting poorer trade-offs across sustainability dimensions. The variation among the top solutions within each strategy is negligible, indicating convergence toward stable regions rather than dispersed local optima. This behaviour demonstrates robustness of the optimisation process and suggests that multiple near-equivalent configurations exist within each weighting regime. Contribution patterns align with the imposed priorities. Single-objective strategies drive dominance of the targeted indicator, while balanced strategies redistribute influence across EC, CE, and LC. In particular, A4 achieves a controlled distribution across the three primary dimensions, and A5 produces the most uniform profile, with no single indicator governing the outcome. Overall, the results highlight that weighting design directly controls both optimisation direction and solution structure, and that balanced formulations provide more stable and practically meaningful outcomes. Agreement between predicted indicators and recalculated results in OneClick LCA further supports the reliability of the framework.

To validate the optimised scenarios, all scenarios were reconstructed in the software, and the corresponding data were extracted. Fig. 8(f) illustrates the residual error between the optimised solutions and the same scenarios reconstructed within the software environment. As

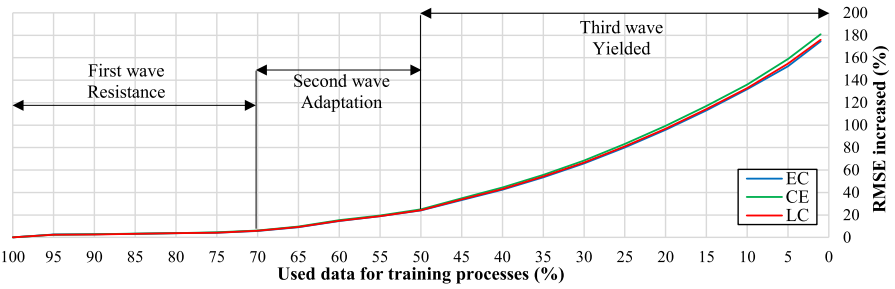


**Note:** "Resistance area": The range of dataset reduction over which model accuracy decreases only gradually, indicating strong robustness and resistance to performance degradation under reduced training data availability; "Adaptation area": the range in which model accuracy decreases approximately linearly with dataset reduction, indicating stable adaptation of the model to decreasing data availability; "Yielded area": the range in which model accuracy decreases more rapidly than the rate of dataset reduction, indicating loss of model stability and reduced generalisation capability under severely limited training data conditions.

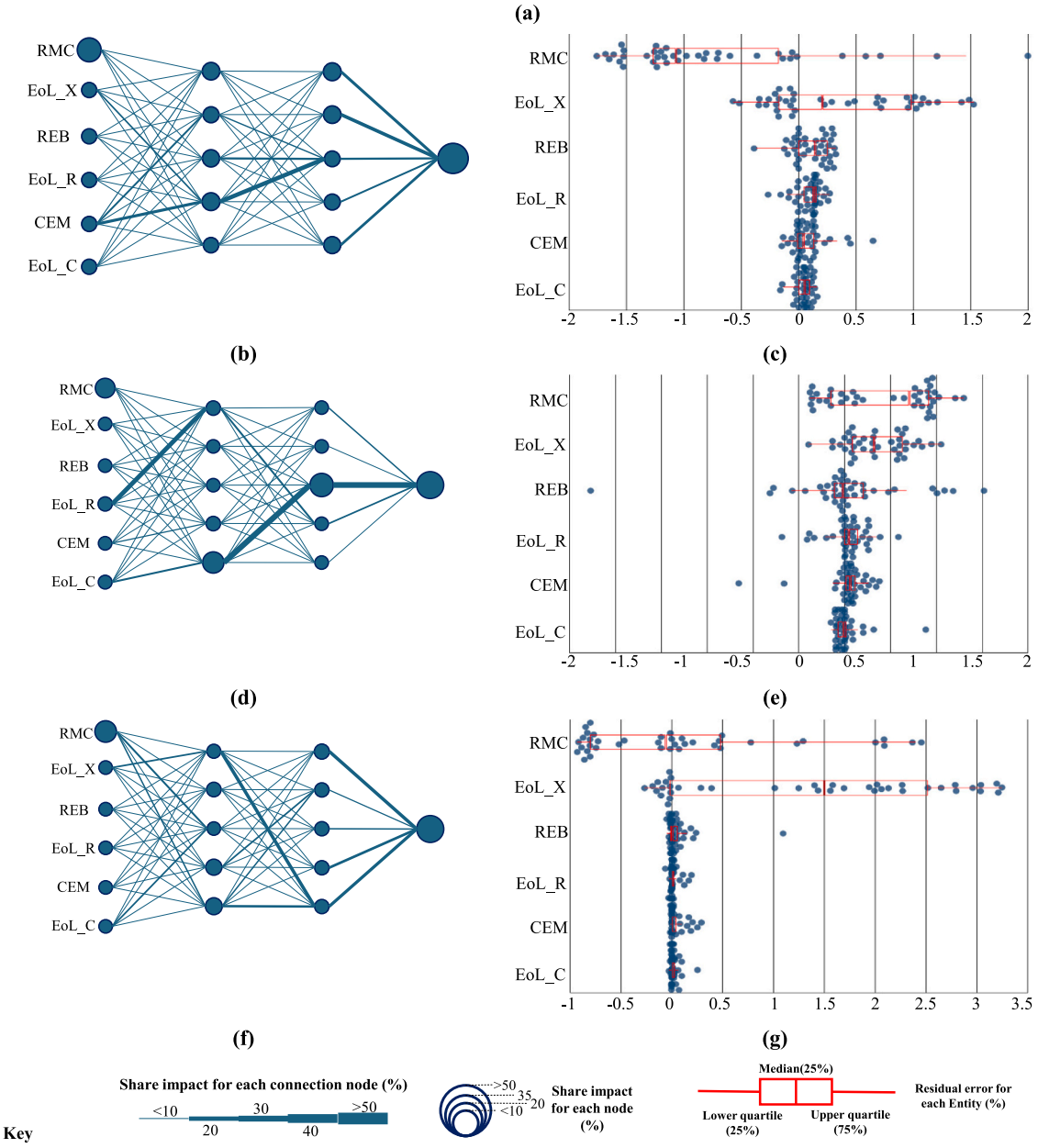


**Fig. 7.** Sensitivity analysis on predication models: (a) uncertainty analysis, (left) LRP analysis, (right) SHAP analysis (%), (b-c) EC, (d-e) CE, (f-g) LC.

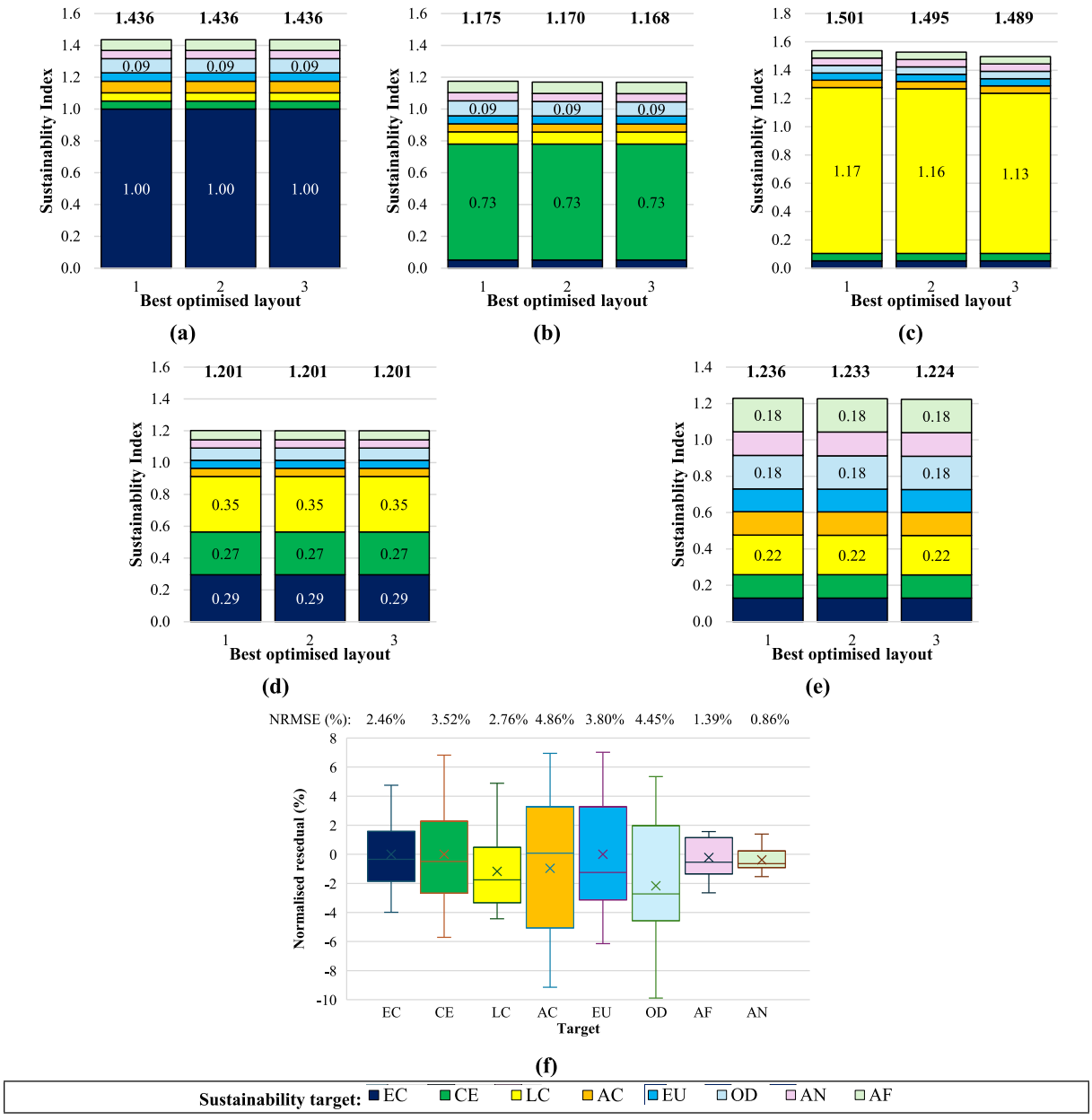


**Fig. 8.** Performance assessment of optimisation model based on share of each sustainability target: (a) Alternative 1, (b) Alternative 2, (c) Alternative 3, (d) Alternative 4, (e) Alternative 5, (f) Normalised residual error in comparison to new built observation results.

shown, residuals for all indicators are centred close to zero, indicating minimal systematic bias between predicted and recalculated results. NRMSE values remain low overall, with AF at 1.39%, EC at 2.46%, and LC at 2.76%, confirming high predictive accuracy for key optimisation targets. Although AN report a relatively higher normalised error, its residual distribution is narrow and consistently slightly negative, indicating localised bias rather than dispersion. In contrast, AC, EU, and OD exhibit wider residual spreads, reflecting greater variability despite moderate error levels. This suggests that error magnitude alone does not fully capture model behaviour, and distribution characteristics must also be considered. Overall, the combined evidence from NRMSE values and residual distributions confirms that the AI-based optimisation framework provides stable and reliable predictions, with strong agreement with recalculated results from OneClick LCA.

The optimisation results were further analysed to assess the influence of weighting strategies on material composition. As shown in Fig. 9, RMC mixtures consistently comprise two to three components, with one dominant share, indicating stable yet flexible mix selection. A similar pattern is observed for REB, where a single reinforcement option governs the composition, with minor secondary contributions. Greater sensitivity is observed in the cement group. The LC-focused strategy (A3) produces a highly concentrated solution, with a single option accounting for about 94% of the mix, whereas balanced strategies (A4-A5) distribute shares more evenly across alternatives, reflecting broader trade-off exploration. EoL selections also vary systematically, aligning with the priorities embedded in each weighting scheme. Overall, the framework generates distinct material configurations that remain practically implementable, while clearly reflecting the imposed sustainability objectives.

The optimisation results provide insight into the interaction between material selection, environmental performance, and life cycle in reinforced-concrete systems. Across all strategies, system behaviour is governed primarily by structural concrete and reinforcement steel, confirming their dominant role in embodied impacts identified in the

| Approach | Material | | | | | | | | |
|---|---|---|---|---|---|---|---|---|---|
| | RMC_1 | RMC_2 | RMC_3 | RMC_4 | RMC_5 | RMC_6 | RMC_7 | RMC_8 | RMC_9 |
| A1 | 0 | 41 | 0 | 0 | 0 | 0 | 59 | 0 | 0 |
| A2 | 0 | 0 | 0 | 80 | 0 | 0 | 20 | 0 | 0 |
| A3 | 0 | 0 | 0 | 30 | 0 | 0 | 20 | 0 | 50 |
| A4 | 0 | 75 | 0 | 0 | 0 | 0 | 25 | 0 | 0 |
| A5 | 0 | 30 | 0 | 54 | 0 | 0 | 16 | 0 | 0 |

(a)

| Approach | Material | | | | | | | | | | | | | | | | | | | |
|---|---|---|---|---|---|---|---|---|---|---|---|---|---|---|---|---|---|---|---|---|
| | REB_1 | REB_2 | REB_3 | REB_4 | REB_5 | REB_6 | REB_7 | REB_8 | REB_9 | REB_10 | REB_11 | REB_12 | REB_13 | REB_14 | REB_15 | REB_16 | REB_17 | REB_18 | REB_19 | REB_20 |
| A1 | 0 | 0 | 0 | 0 | 0 | 0 | 0 | 0 | 15 | 0 | 0 | 0 | 0 | 0 | 0 | 85 | 0 | 0 | 0 | 0 |
| A2 | 0 | 80 | 5 | 0 | 0 | 0 | 0 | 0 | 0 | 0 | 15 | 0 | 0 | 0 | 0 | 0 | 0 | 0 | 0 | 0 |
| A3 | 0 | 75 | 10 | 0 | 0 | 0 | 0 | 0 | 0 | 0 | 0 | 0 | 0 | 0 | 0 | 15 | 0 | 0 | 0 | 0 |
| A4 | 0 | 0 | 10 | 85 | 5 | 0 | 0 | 0 | 0 | 0 | 0 | 0 | 0 | 0 | 0 | 0 | 0 | 0 | 0 | 0 |
| A5 | 0 | 0 | 0 | 85 | 0 | 0 | 5 | 0 | 0 | 0 | 0 | 0 | 0 | 0 | 10 | 0 | 0 | 0 | 0 | 0 |

(b)

| Approach | Material | | | | | | | | |
|---|---|---|---|---|---|---|---|---|---|
| | CEM_1 | CEM_2 | CEM_3 | CEM_4 | CEM_5 | CEM_6 | CEM_7 | CEM_8 | CEM_9 |
| A1 | 0 | 0 | 0 | 26 | 46 | 28 | 0 | 0 | 0 |
| A2 | 0 | 60 | 30 | 0 | 0 | 0 | 0 | 10 | 0 |
| A3 | 0 | 0 | 94 | 0 | 6 | 0 | 0 | 0 | 0 |
| A4 | 0 | 0 | 42 | 0 | 56 | 2 | 0 | 0 | 0 |
| A5 | 0 | 54 | 44 | 0 | 0 | 0 | 0 | 2 | 0 |

(c)

| Approach | EoL | | |
|---|---|---|---|
| | X | R | C |
| A1 | Crushed | Recycling | Backfilling |
| A2 | Crushed | Recycling | Reuse |
| A3 | Landfilling | Reuse | Backfilling |
| A4 | Crushed | Reuse | Backfilling |
| A5 | Crushed | Recycling | Reuse |

(d)

>50% 10-50% <10%

**Fig. 9.** Material analysis on the optimised approaches: (a) RMC, (b) REB, (c) CEM, (d) EoL.

benchmark LCA. When environmental indicators are prioritised, solutions favour modified concrete compositions and alternative reinforcement specifications that reduce embodied impacts while preserving structural equivalence. In contrast, the cost-driven strategy (A3) shifts the solution toward cost-efficient options, producing highly concentrated material selections and reduced diversity. The circularity-focused strategy (A2) introduces stronger influence of EoL routing, promoting configurations that enhance recovery performance while maintaining competitive environmental outcomes.

Balanced strategies (A4-A5) generate intermediate solutions, moderating environmental, circularity, and cost objectives without dominance of a single criterion. Overall, the results demonstrate that the framework enables systematic exploration of LCA–LC trade-offs and identifies practically implementable configurations that improve environmental performance without disproportionate cost penalties, supporting informed material optimisation at early design stages. From a policy perspective, the proposed framework provides a practical tool for supporting emerging regulations on embodied carbon and resource efficiency in the built environment.

By enabling systematic evaluation of material configurations at the design stage, the framework can assist in aligning building projects with national and international targets related to carbon reduction, circular economy, and sustainable construction. In particular, it supports early-stage decision-making required by standards such as EN 15978 and evolving regulatory initiatives targeting whole-life carbon assessment. Furthermore, the ability to quantify trade-offs between environmental impact, circularity, and cost provides a basis for more informed policy development, including material efficiency strategies, low-carbon procurement guidelines, and performance-based building regulations.

## 4. Conclusion

This study developed an integrated artificial intelligence–assisted framework for exploring and optimising construction material configurations using LCA, circularity metrics, and LC within a unified modelling workflow. A reinforced-concrete office building case study was used to generate a large set of technically feasible material scenarios, which were then used to train predictive models and support sustainability-oriented optimisation. Unlike conventional scenario-based LCA studies, the proposed optimisation framework allows the simultaneous adjustment of multiple material shares, enabling the generation of new material combinations within defined feasibility boundaries rather than restricting analysis to predefined substitution pathways.

For the investigated case study, the underlying LCA calculations remain predominantly linear; however, the proposed framework addresses the optimisation and decision-support challenges associated with exploring large material-design spaces rather than the calculation of LCIA indicators themselves. The main findings of the study can be summarised as follows:

- A scenario library of 1500 technically feasible material configurations was generated by varying concrete mixes, reinforcement steel production routes, cement formulations, and EoL pathways.
- The developed predictive models reproduced the LCA outputs with very high accuracy. Across all sustainability indicators, coefficients of determination generally exceeded 98–99%, while prediction errors remained low in both single-variation and multivariate validation scenarios.
- The optimisation framework demonstrated that sustainability outcomes are strongly influenced by the weighting strategy applied to the SI. Different optimisation strategies produced distinct trade-offs between environmental performance, circularity, and LC.
- The optimisation process consistently converged toward stable regions of the material design space, indicating robust algorithm performance and well-defined sustainability optima.
- Material configuration analysis revealed that only a limited number of dominant material options govern sustainability performance within each group. In particular, optimised mixtures typically relied on two to three primary alternatives for concrete, reinforcement steel, and cement.
- The results demonstrate that combining predictive modelling with optimisation enables efficient exploration of complex material design spaces while preserving engineering feasibility and constructability constraints.

Although, the framework provides a scalable decision-support approach for early-stage sustainable material selection, enabling designers to evaluate LCA and LC trade-offs and identify feasible material optimisation strategies, following limitations should be acknowledged:

- The generation of large scenario libraries currently requires manual modelling within the LCA software environment. Constructing thousands of scenarios therefore becomes time-consuming and impractical without automation.

- The framework relies on available environmental product declarations (EPDs) and generic database records. The underlying environmental datasets were adopted as provided by the software and were not independently verified.
- The case study focused on a single reinforced-concrete building configuration, which may limit the direct generalisation of results to other building typologies or structural systems.
- This study is limited to a single office-building case study and does not explicitly consider variations across urban density, residential and commercial building typologies, occupancy patterns, gross floor area per capita, or differences in built-form characteristics between detached housing, apartment buildings, and other urban development configurations. Consequently, broader planning-scale implications related to population density, housing distribution, and per-capita environmental impacts were beyond the scope of the present analysis. Future work should therefore extend the proposed framework to multiple building typologies and urban contexts to support wider planning-scale sustainability assessment and comparison of environmental impacts across different built-form and occupancy conditions.
- Although the proposed framework provides a scalable and flexible approach for AI-assisted material optimisation at the building level, the present study is limited to a single reinforced-concrete office-building case study and does not explicitly account for variations in urban density, residential and commercial building typologies, occupancy distribution, gross floor area per capita, or regional built-form characteristics. Consequently, broader planning-scale implications associated with different urban-development patterns and building-stock compositions were beyond the scope of the current investigation. Future research should therefore extend the proposed framework toward multi-building and planning-scale applications, enabling comparative sustainability assessment across urban, sub-urban, and rural contexts while incorporating variations in building typology, occupancy characteristics, and regional material-consumption patterns to better support urban and regional sustainability planning.

## Declaration of competing interest

The authors declare that they have no known competing financial interests or personal relationships that could have appeared to influence the work reported in this paper.

## Acknowledgement

The authors acknowledge that the conceptual foundation of this study is supported by UH impact Policy Support Fund 2025/2026. In this regard, the authors wish to extend their appreciation to Engineers Reeya Khan and Connor Wilding for their technical contributions and for establishing the preliminary framework that informed the further development of this research.

## Appendix A. Supplementary data

Supplementary data to this article can be found online at https://doi.org/10.1016/j.eiar.2026.108582.

## Data availability

No data was used for the research described in the article.

## References

AbouHamad, M., Abu-Hamd, M., 2019. Framework for construction system selection based on life cycle cost and sustainability assessment. J. Clean. Prod. 241, 118397.
Aghdam, M.N., Dixit, M.K., 2026. A systematic review of methods and frameworks integrating environmental sustainability and resilience in building design and construction. Build. Environ. 293, 114381.
Ahmadi, M., Piadeh, F., Hosseini, M.R., Zuo, J., Kocaturk, T., 2024. Unravelling building sector carbon mechanisms: critique and solutions. Renew. Sustain. Energy Rev. 205, 114873.
Ahmadi, M., Pournaghshband, A., Piadeh, F., Hosseini, R., 2025. Circularity-based embodied carbon performance in building design. J. Clean. Prod. 518, 145909.
Ajayi, A.B., Zhang, Y., Mostafa, H., Chen, L., 2025. Application of ANN-ML in evaluating indoor thermal comfort of trio-typology residential building. Urban Clim. 64, 102625.
Alwan, Z., Jones, P., Holgate, P., 2017. Strategic sustainable development in the UK construction industry through the framework for strategic sustainable development using building information modelling. J. Clean. Prod. 140, 349–358.
Ashkbous, M., Ghorbani, E., Keivanpour, S., 2026. Artificial intelligence for eco-design: a systematic review. Adv. Eng. Inform. 69 (C), 103989.
Azghandi, M.N., Shojaei, A.A., Lotfi, H., 2025. Hybrid PSO-SFLA with fuzzy optimization for multi-area dynamic economic load dispatch and demand response. Energy 360 (3), 100021.
Barbhuiya, S., Das, B.B., 2023. Life cycle assessment of construction materials: methodologies, applications and future directions for sustainable decision-making. Case Stud. Constr. Mater. 19, p. 02326.
Bibri, S., Huang, J., 2025. AI and AI-powered digital twins for smart, green, and zero-energy buildings: a systematic review of leading-edge solutions for advancing environmental sustainability goals. Environ. Sci. Ecotechnol. 28, 100628.
British Standards Institution (BSI), 2012. BS EN 15978:2011 Sustainability of Construction Works - Assessment of Environmental Performance of Buildings - Calculation Method. BSI, London, UK.
British Standards Institution (BSI), 2019. BS EN 15804:2012+A2:2019 Sustainability of Construction Works - Environmental Product Declarations - Core Rules for the Product Category of Construction Products. BSI, London, UK.
Cabeza, L.F., Rincón, L., Vilariño, V., Pérez, G., Castell, A., 2014. Life cycle assessment (LCA) and life cycle energy analysis (LCEA) of buildings and the building sector: a review. Renew. Sustain. Energy Rev. 29, 394–416.
Carreira-Barral, I., García-Moral, A., Iñigo-Martínez, M., Díez-Hernández, J., Ibáñez, J., Alonso-Terán, M., De La Fuente, P., Barros, R., Martel-Martín, S., 2026. A five-indicator methodology for early-stage sustainable selection of metal scraps and raw materials: application in the steel industry. Environ. Impact Assess. Rev. 119, 108364.
Carvalho, J.P., Villaschi, F.S., Bragança, L., 2021. Assessing life cycle environmental and economic impacts of building construction solutions with BIM. Sustainability 13 (16), 8914.
Chamlal, H., Kamel, H., Ouaderhman, T., 2024. A stacking ensemble classifier with GAN-SFLA for improved diagnosis in imbalanced healthcare data. Procedia Computer Science 251, 494–501.
Dai, R., Zhang, G., Li, S., Zhang, R., Bai, G., 2026. An AI-driven MABM–BIM–DL framework for energy consumption prediction in three representative types of urban public buildings in Wuhan. Sustain. Cities Soc. 144, 107434.
Dai, S., 2026. A state-of-the-art review of the life cycle assessment of rammed earth building construction. Energ. Buildings 350, 116643.
Devaki, H., Shanmugapriya, S., 2022. Life cycle assessment on construction and demolition waste management approaches: a review. Material Today Processing 65, 764–770.
Dewi, O.C., Nasruddin, N., Salsabila, N.D., Rahmasari, K., Khairunnisa, G., 2025. Building circularity potential for post-disaster housing: LCA, cost evaluation, and material optimization. Circular Economy 4 (2), 100141.
Dinh, T.H., Hieu, D., Götze, U., 2020. Integration of sustainability criteria and life cycle sustainability assessment method into construction material selection in developing countries: the case of Vietnam. International Information Engineering Technology Association 15 (8), 1145–1156.
Dong, Y., Jaillon, L., Chu, P., Poon, C.S., 2023. Life cycle sustainability assessment of building construction: a comparative case study in China. J. Clean. Prod. 388, 135843.
Drewniok, M.P., Dunant, C.F., Allwood, J.M., Ibell, T., Hawkins, W., 2023. Modelling the embodied carbon cost of UK domestic building construction: today to 2050. Ecol. Econ. 205, 107725.
Gachkar, D., Gachkar, S., Ghofrani, E., Martínez, A.G., Bahón, C.A., 2025. Automating data integration for construction life cycle assessment using fuzzy matching and supervised learning. Autom. Constr. 178, 106381.
Galimshina, A., Moustapha, M., Hollberg, A., Padey, P., Lasvaux, S., Sudret, B., Habert, G., 2022. Bio-based materials as a robust solution for building renovation: a case study. Appl. Energy 316, 119102.
Geissdoerfer, M., Savaget, P., Bocken, N.M.P., Hultink, E.J., 2017. The circular economy – a new sustainability paradigm? J. Clean. Prod. 143, 757–768.
Ghaffarianhoseini, A., Ghaffarianhoseini, A., Tookey, J., Omrany, H., Fleury, A., Naismith, N., 2021. Sustainable material choice for construction projects using life cycle sustainability assessment. J. Build. Eng. 43, 102848.
Guo, D., Di Modica, P., La Rosa, A.D., 2025. A semantic-enriched LCI database for the embodied environmental evaluation of buildings through knowledge graph technologies. IFAC-PapersOnLine 59 (10), 2474–2478.
Häfliger, I.F., John, V., Passer, A., Lasvaux, S., Hoxha, E., Saade, M.R., Habert, G., 2017. Buildings environmental impacts' sensitivity related to LCA modelling choices of construction materials. J. Clean. Prod. 156, 805–816.
Hassan Khan, M.A., Ahmed, A., Ali, T., Qureshi, M.Z., Islam, S., Ahmed, H., Ajwad, A., Khan, M.A., 2025. Comprehensive review of 3D printed concrete, life cycle

assessment, AI and ML models: materials, engineered properties and techniques for additive manufacturing. Sustain. Mater. Technol. 43, 01164.
Hernández, H., Ossio, F., Silva, M., 2023. Assessment of sustainability and efficiency metrics in modern methods of construction: a case study using a life cycle assessment approach. Sustainability 15 (7), 6267.
Hu, M., Avval, S., He, J., Yue, N., Groves, R., 2025. Explainable artificial intelligence study on bolt loosening detection using lamb waves. Mech. Syst. Signal Process. 225, 112285.
Huang, B., Zhang, H., Ullah, H., Lv, Y., 2025. BIM-based embodied carbon evaluation during building early-design stage: a systematic literature review. Environ. Impact Assess. Rev. 112, 107768.
International Organization for Standardization (ISO), 2006. ISO 14040:2006 Environmental Management — Life Cycle Assessment — Principles and Framework. ISO, Geneva, Switzerland.
International Organization for Standardization (ISO), 2015. ISO 14000:2015 Environmental Management Systems — Fundamentals and Vocabulary. ISO, Geneva, Switzerland.
Iqbal, N., Shabbir, K., Noureldin, M., 2025. A novel explainable AI-based design optimization framework to estimate sustainability and economic impacts of reinforced concrete structures. Mach. Learn. Appl. 22, 100760.
Kang, F., Lin, H., Zhou, Z., Ren, Y., Li, X., Wang, J., 2026. Uncertainty-aware hybrid modelling for spatial thermal forecasting in historic buildings with incomplete structural information. J. Build. Eng. 119, 115231.
Kebede, R., Oetsch, J., Johansson, P., Moscati, A., 2026. AI-driven decision support using digital product passports for end-of-life management in the circular built environment. Procedia Computer Science 277, 3361–3369.
Kirchherr, J., Reike, D., Hekkert, M., 2017. Conceptualizing the circular economy: an analysis of 114 definitions. Resour. Conserv. Recycl. 127, 221–232.
Li, S., Sung, Y., 2025. Type-based mixture of experts and semi-supervised multi-task pre-training for symbolic music. Expert Syst. Appl. 292, 128613.
Lighittha, P., Prithivraj, S., Sangeetha, R., 2026. FireAntGA-ImmunoModel: an explainable bio-inspired hybrid framework for optimized immunodiagnostic classification. Results Eng. 29, 109267.
Lima, M.S.S., Duarte, S., Exenberger, H., Fröch, G., Flora, M., 2024. Integrating BIM-LCA to enhance sustainability assessments of constructions. Sustainability 16, 1172.
Liu, S., Qian, S., 2019. Towards sustainability-oriented decision making: model development and its validation via a comparative case study on building construction methods. Sustain. Dev. 27, 860–872.
Maria, A., Eyckmans, J., Acker, K., 2018. Downcycling versus recycling of construction and demolition waste: combining LCA and LCC to support sustainable policy making. Waste Manag. 75, 3–21.
Mohtashami, N., Streblow, R., Frisch, J., Müller, D., 2026. We May Be Retrofitting Wrong: How LCA Exposes Hidden Trade-Offs of Carbon Footprint and Costs of Optimal Energy Retrofitting Upgrades.
Moustafa, Z., Luqman, M., Wuni, I.Y., Zami, M., Asif, M., 2026. An integrated system dynamics-AHP-TOPSIS framework for green innovation in sustainable building materials: application to a rapidly urbanizing economy. Results Eng. 29, 108998.
Nouri, A., Hu, M., 2025. Democratizing environmental impact assessment: an AI-augmented framework for sustainable building design. iScience 29 (2), 1–12, 114589.
Offie, I., Piadeh, F., Behzadian, K., Campus, L., Rokiah, Y., 2023. Development of an artificial intelligence-based framework for biogas generation from a Micro anaerobic digestion plant. Waste Manag. 158, 66–75.
Parece, S., Resende, R., Rato, V., 2025a. BIM-based life cycle assessment: a systematic review on automation and decision-making during design. Build. Environ. 282, 113248.
Parece, S., Resende, R., Rato, V., 2025b. Stakeholder perspectives on BIM-LCA integration in building design: adoption, challenges, and future directions. Build. Environ. 284, 113434.
Pasanen, P., 2025. Generic materials data production at one click LCA. One click LCA resources [online] available at https://oneclicklca.com. <retrieved 10/05/2026>.
Peng, J., Khuat, T., Musial, K., Gabrys, B., 2026. Machine learning methods for small data and upstream bioprocessing applications: a comprehensive review. Biotechnol. Adv. 87, 108749.
Piadeh, F., Pournaghshband, A., 2026. Application of artificial intelligence in circularity assessment of building waste materials: a comprehensive review of recent advances and future directions. Circ. Econ. Sustain. 6 (152), 893.
Piadeh, F., Ahmadi, M., Behzadian, K., 2020. A novel planning policy framework for the recognition of responsible stakeholders in the of industrial wastewater reuse projects. Journal of Water Policy 24 (9), 1541–1558.
Piadeh, F., Behzadian, K., Chen, A., Kapelan, Z., Rizzuto, J., Campos, L., 2023. Enhancing urban flood forecasting in drainage systems using dynamic ensemble-based data mining. Water Res. 247, 120791.
Piadeh, F., Offie, I., Behzadian, K., Bywater, A., Campos, L., 2024. Real-time operation of municipal anaerobic digestion using an ensemble data mining framework. Bioresour. Technol. 392, 130017.
Plociennik, C., Watjanatepin, P., Acker, K., Ruskowski, M., 2025. Life cycle assessment of artificial intelligence applications: research gaps and opportunities. Procedia CIRP 135, 924–929.
Rizzo, S.A., 2025. To be artificial intelligence for sustainability or not to be sustainable artificial intelligence. Renew. Sustain. Energy Rev. 223, 116063.
Sabet, H., Sadri, Moghaddam S., Piadeh, F., 2025. Rapid sustainability assessment of sludge management technologies for industrial scale-up. Sustainable Prod. Consumption 53, 163–176.
Sandanayake, M., Bouras, Y., Vrcelj, Z., 2022. A feasibility study of using coffee cup waste as a building material - life cycle assessment and multi-objective optimisation. J. Clean. Prod. 339, 130498.
Serrano-Baena, M.M., Ruiz-Díaz, C., Boronat, P.G., Mercader-Moyano, P., 2023. Optimising LCA in complex buildings with MLCAQ: a BIM-based methodology for automated multi-criteria materials selection. Energ. Buildings 294, 113219.
Sesana, M.M., Dell'Oro, P., Salvalai, G., Gervasio, H., 2026. Building life cycle assessment and digital technologies: a bibliometric and systematic literature review and recent advances on their integration to boost the decarbonization of the construction sector. Energy Build. 352, 116833.
Shi, Y., Cao, X., Yang, Z., Li, M., Yu, X., Yang, X., 2026. Multi-objective optimization of window retrofit for dormitory buildings under material circularity uncertainties: a robust surrogate-assisted framework. Journal of Building Engineering 293, 114372, 123, p.115941.
Valipour, A., Manesh, M.S., Balali, A., 2025. Sustainable material selection for the reconstruction of historical buildings using building information modeling (BIM) in developing countries. Sustainable Cities and Society: Advances 1 (1), 100004.
Vandersmissen, B., Oramas, J., 2024. On the coherency of quantitative evaluation of visual explanations. Comput. Vis. Image Underst. 241, 103934.
Vilutiene, T., Kumetaitis, G., Kiaulakis, A., Kalibatas, D., 2020. Assessing the sustainability of alternative structural solutions of a building: a case study. Buildings 10 (2), 36.
Xi, H., Shao, Z., Hensher, D., Nelson, J., Chen, H., Wijayaratna, K., 2025. A multi-task transformer with mixture-of-experts for personalized periodic predictions of individual travel behavior in multimodal public transport. Transportation Research Part C: Emerging Technologies 179, 105287.
Yadav, A.A., Hirekhan, S.G., Bhandari, P.S., Bhagat, R.M., Ranit, A.B., Shelare, S., Soudagar, M.E.M., Sharma, S., Raja, V.K.B., Mahapatro, A., Singh, S., Kumar, A., Massoud, E.E., 2025. AI-driven sustainable concrete mix design: hybrid deep Q-learning and genetic algorithms-based multi-objective machine learning optimizations for high structural strength, low cost, and low carbon footprints. Structures 82, 110443.